Supplemental Notes

SN1. Visualizing location of platform-discordant protein-altering genetic variants in protein structures

Upon visualizing consequences of each of the platform-discordant protein altering variants (PAVs) in AlphaFold predicted protein structures, we observed the majority of platform-discordant PAVs encode amino-acid changes on the surface of the protein, supporting the notion that these variants may reflect interference with affinity probe binding (**Figure S21-37**).

SN2. Impact of adjustment for platform-discordant PAVs pQTL on inter-platform correlation (across all probe pairs)

For the 19 proteins associated with a platform-discordant PAV *cis*-pQTL across all probe pairs (**Table S5; Figure S5**), we adjusted each platform's measures for copies of the PAV, and computed inter-platform correlation estimates with residual measures. Prior to PAV-adjustment, the mean inter-platform correlation estimate for these proteins was 0.37, with estimates ranging from -0.39 to 0.66. Post PAV-adjustment, the mean inter-platform correlation increased to 0.51, with estimates ranging from 0.15 to 0.76 (**Table S5; Extended Data Figure 6**).

SN3. Adjustment for platform-discordant PAV pQTL in *cis*-pQTL mapping

On SomaScan, 2 *cis*-pQTL signals, for 2 unique proteins (ACP1 and CPPED1), become significant only upon using PAV-adjusted protein measures in pQTL mapping (**Table S22**, **Figure S7-S8**).

Additionally, a subset of 8 signals for 8 proteins on SomaScan (APOL1, APOE, CLU, CTSH, KDR, PGLYRP2, PLAUR, RNASE6) (**Table S20**), and 4 signals for 4 proteins on Olink (CTSH, CTSS, HNMT, and PILRA) increased in significance following adjustment for platform-discordant PAV (**Table S21**), (**Figures S9-S17)**. For example, when mapping pQTL using PAV-adjusted PILRA measures, an alternate non-coding genetic signal, driven by

chr7:10048786:C:G, exhibited increased significance for Olink's PILRA measures (Pre-PAV Adjustment P=3.70*10^{-15}, Post-PAV Adjustment P=1.67*10^{-23}) (**Extended Data Figure 8)**. Similarly, mapping pQTL with suPAR measures adjusted for the platform-discordant PAV results in increased significance of an independent, platform-concordant signal driven by chr19:43652320:T:C on SomaScan (Pre-PAV Adjustment P=2.94*10^{-14}, Post-PAV Adjustment P=1.49*10^{-21}) (**Extended Data Figure 9**).

SN4. Additional examples of ancestry-differentiated, platform-discordant PAV *cis*-pQTL

In addition to suPAR, two additional proteins -- apolipoprotein 1 (APOL1) and Calcineurin Like Phosphoesterase Domain Containing 1 (CPPED1) – are associated with platform-discordant PAVs most prevalent among participants clustering with the African (AFR) ancestry reference population.

APOL1

APOL1 associates with an ancestry-differentiated, platform-discordant PAV (rs2239785, chr22:36265284:G:A, Glu166Lys, EAF X^2=449.8, X^2 p=3.47*10^{-97}) **(Figure S10, Figure S28)** common across all ancestry clusters contributing to this study, but most common among individuals clustering with the African ancestry reference (EAF=0.63). Following adjustment for this PAV, correlation improved to the largest extent among individuals in the AFR ancestry group (Pearson's r Pre-PAV Adjustment=0.34, Pearson's r Post-PAV Adjustment = 0.47). **(Figure S19)** Additionally, pQTL mapping using APOL1 measures adjusted for copies of the platform-discordant PAV resulted in improved strength of a *cis*-pQTL association driven by a noncoding variant, chr22:36251719:A:T **(Figure S10).**

Given the proximity of rs2239785 to APOL1 G1 and G2 kidney disease genotype risk factors, we further examined whether rs2239785 was independent of these variants by adjusting for APOL1 risk haplotypes in pQTL mapping (with non-PAV adjusted APOL1 measures). While

adjustment for APOL1 G1/G2 risk haplotype slightly attenuated the PAV signal, the signal was still present, suggesting independence from known risk variants in the region **(Figure S20).**

CPPED1

CPPED1 associates with an ancestry-differentiated, platform discordant PAV (rs3748976, chr16:12803721:G:T, A19D, EAF X^2=299.2, EAF X^2 p=1.45*10^{-64}) **(Figure S8, Figure S30)** most common among individuals of AFR ancestry (EAF=0.60). While adjustment for this PAV improves CPPED1 measures across all participants from inter-platform Pearson's r -0.14 to 0.47, interestingly, the largest improvement is not among individuals of AFR ancestry (Pearson's r improvement from -0.06 to 0.27 post-adjustment), but rather, individuals clustering with AMR references (r improvement from -0.06 to 0.45 post-adjustment), suggesting interplay of other genetic variants or technical/environmental factors **(Figure S21)**. However, adjustment for this platform-discordant PAV results in a new *cis*-pQTL signal on SomaScan, led by chr16:12768150:A:C (PAV-Adjusted lead variant p-value=1.78*10^{-55}) (**Figure S8**).

SN5. Adjustment for platform-specific pQTL

Adjustment for platform specific PAVs also, on average, modestly improved assay correlation (mean difference 5.1E-02 for 256 Olink-specific PAVs, mean difference 1.5E-02 for SomaScan specific PAVs; see **Figure S22**), but differences were generally minor compared to the large improvements seen for the smaller number of platform discordant PAVs. The overall impact of using protein measures adjusted for platform-specific PAV in epidemiological models was minimal; the correlation of phenotypic effect sizes obtained from models with unadjusted vs. adjusted measures was similar (**Figure S23; S24**). Full results from these analyses can be found in **Table S23** and **Table S24**. Similarly, adjustment for proteins associated with SomaScan-specific pleiotropic *trans*-pQTL did not change inter-platform correlation (**Figure S25**; **Table S25**).

SN6. Summary table and extended data

A key summarizing correlation, per-ancestry correlation estimates, and pQTL summary statistics per platform can be found in **Supplemental Table 26.** pQTL and LOD result summaries and credible sets corresponding to results from considering all probes for the 2,157 platform overlapping proteins can be found in the **Extended Data Tables**.

Supplemental Methods

Visualizing location of platform-discordant PAVs in protein structures

Protein FASTA sequences were obtained from UniProt (www.uniprot.org/)[1] and modified to reflect the isoform encoded by each platform-discordant PAV. FASTA sequences were then input into the AlphaFold Server (https://alphafoldserver.com/) [2] to obtain predicted structure models. Structures were visualized and images were generated in Pymol [3].

Adjustment for APOL1 G1 and G2 kidney disease risk alleles

APOL1 G1 (rs73885219, chr:36269595:AATAATT:A) and G2 (rs71785313, chr22:36265860:A:G) risk alleles were extracted from TOPMed Freeze 8 (due to missingness in TOPMed Freeze 10). G1 was coded as 0, 1, or 2, based on copies of the minor allele (the deletion). Similarly, G2 was coded as 0, 1, or 2, based on copies of the minor allele (the G allele). The following allele combinations were considered as high risk: G1=1 and G2=1; or G1=2 and G2=0; or G1=0 and G2=2. All other combinations were considered low risk. Risk status was adjusted for as a covariate in APOL1 pQTL mapping (performed as reported in main analysis methods). Resulting pQTL association statistics were used to determine the robustness of the platform-discordant PAV signal to the APOL1 risk alleles.

Supplemental References

1. UniProt Consortium. Uniprot: the universal protein knowledgebase in 2025. *Nucleic Acids Res.* (2024) doi:10.1093/nar/gkae1010.

2. Jumper, J. *et al.* Highly accurate protein structure prediction with AlphaFold. *Nature* 596, 583–589 (2021).

3. Schrödinger, L., & DeLano, W. *PyMOL*. (2020).

(A) SomaScan 7k

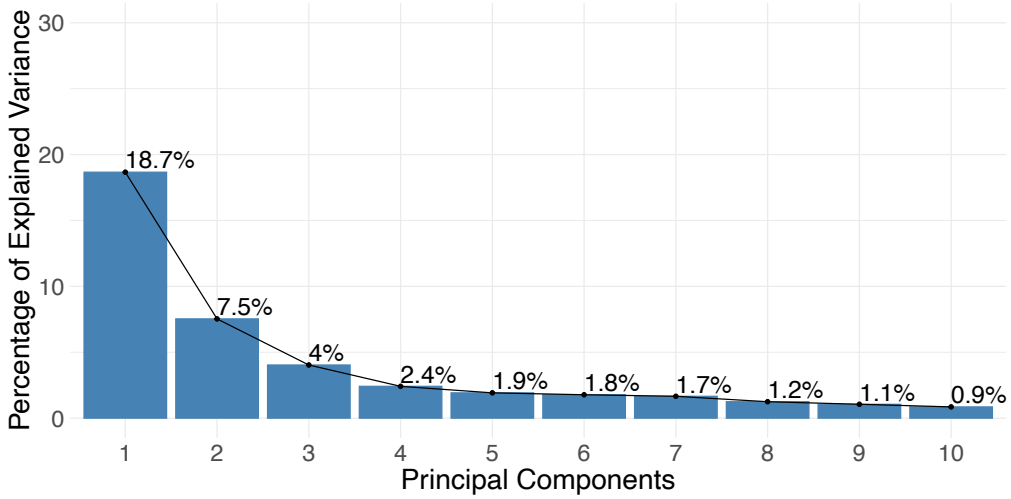

(B) Olink Explore 3072

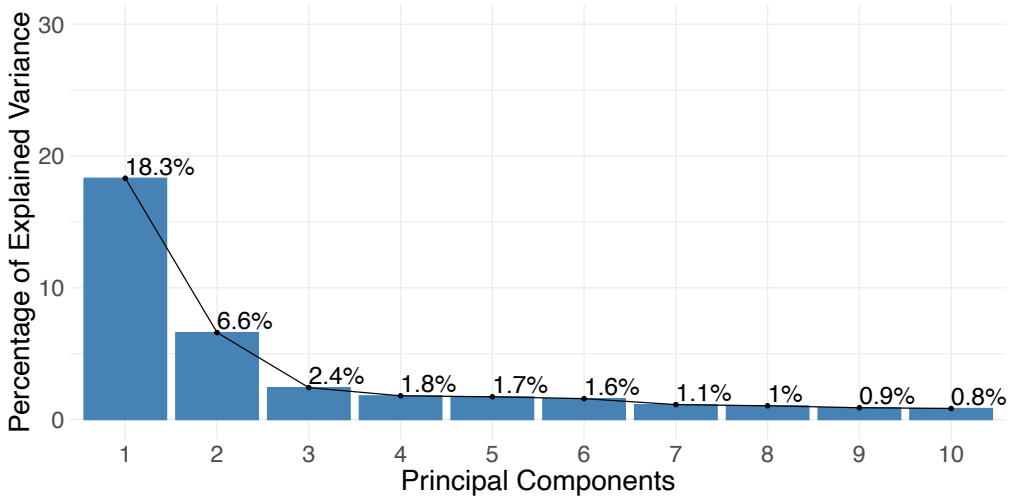

Supplemental Figure 1. Scree plot depicting percentage of variance explained by protein principal components on (A) SomaScan 7k (using sample measures with adaptive-normalization by maximum likelihood) and (B) Olink Explore 3072 in 1,923 MESA participants. Principal component analyses were performed across all proteins analyzed on each platform.

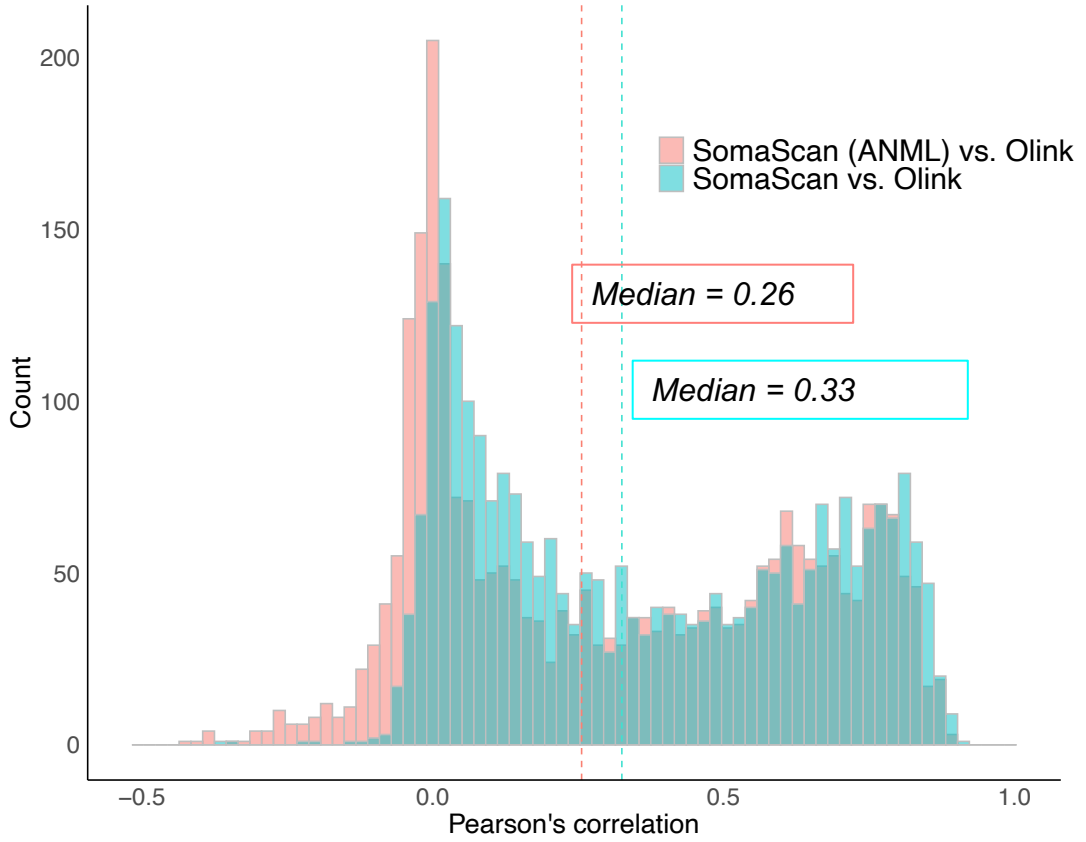

	Minimum	Median	Mean	IQR	Maximum
SomaScan (ANML) vs. Olink	-0.42	0.26	0.31	[0.01, 0.61]	0.90
SomaScan vs. Olink	-0.37	0.32	0.37	[0.08, 0.65]	0.91

Supplemental Figure 2. Inter-platform Pearson's correlation estimates for 2,708 SomaScan 7k and Olink Explore 3072 affinity probe pairs, corresponding to 2,157 UniProt targets assayed on both platforms. Correlation (Pearson's r) estimates from comparison of SomaScan measures with adaptive-normalization (ANML-SMP) performed across all samples shown to Olink measures displayed in pink, whereas estimates from comparison of SomaScan measures with ANML performed in quality control samples only (ANML-QC) to Olink measures shown in blue.

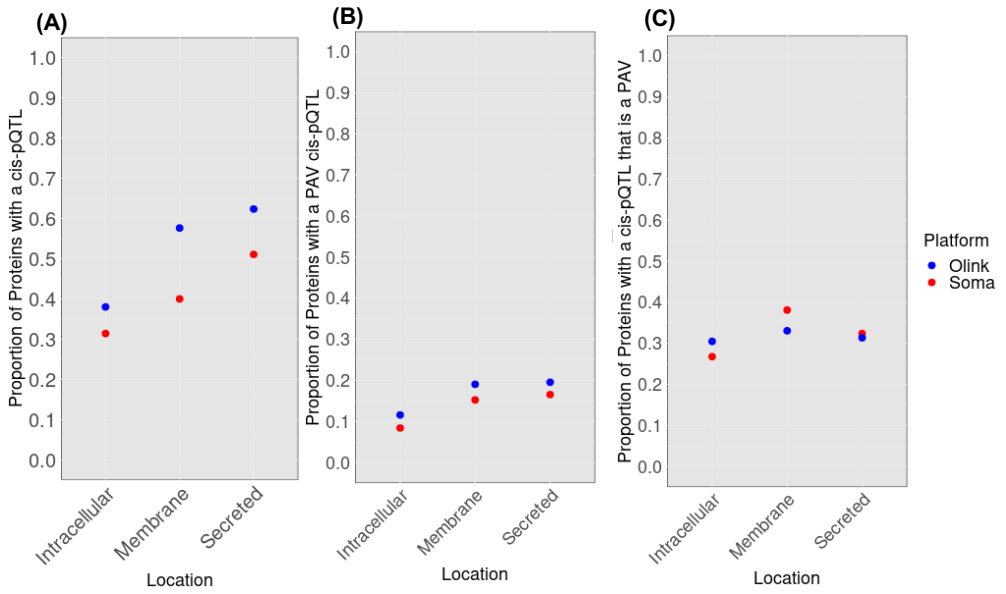

(D)

Location	Total N Proteins	Platform	N Proteins with *cis*-pQTL	Proportion of Proteins with *cis*-pQTL (A)	N Proteins with PAV	Proportion of Proteins with PAV (B)	Proportion of Proteins with a *cis*-pQTL that contain a PAV (C)
Intracellular	1226	Soma	385	0.31	103	0.084	0.27
Intracellular	1226	Olink	466	0.38	142	0.12	0.30
Membrane	210	Soma	84	0.40	32	0.15	0.38
Membrane	210	Olink	121	0.58	40	0.19	0.33
Secreted	701	Soma	358	0.51	116	0.17	0.32
Secreted	701	Olink	437	0.62	137	0.20	0.31

Supplemental Figure 3. Protein *cis*-pQTL status according to subcellular location. The 2,157 proteins measured on both SomaScan 7k and Olink Explore 3072 were classified as intracellular, membrane, or secreted (according to Human Protein Atlas reported location, see Methods). Within each category and platform, we determined the proportion of proteins (A) associated with a significant *cis*-pQTL, (B) associated with a *cis*-pQTL containing a PAV, and (C) associated with a *cis*-pQTL PAV relative to total number of proteins associated with a *cis*-pQTL. Counts and proportions are reported in (D). Significant *cis*-pQTL were detected for larger proportions of secreted proteins on each platforms, but similar proportions of PAV associations were observed for proteins in each category.

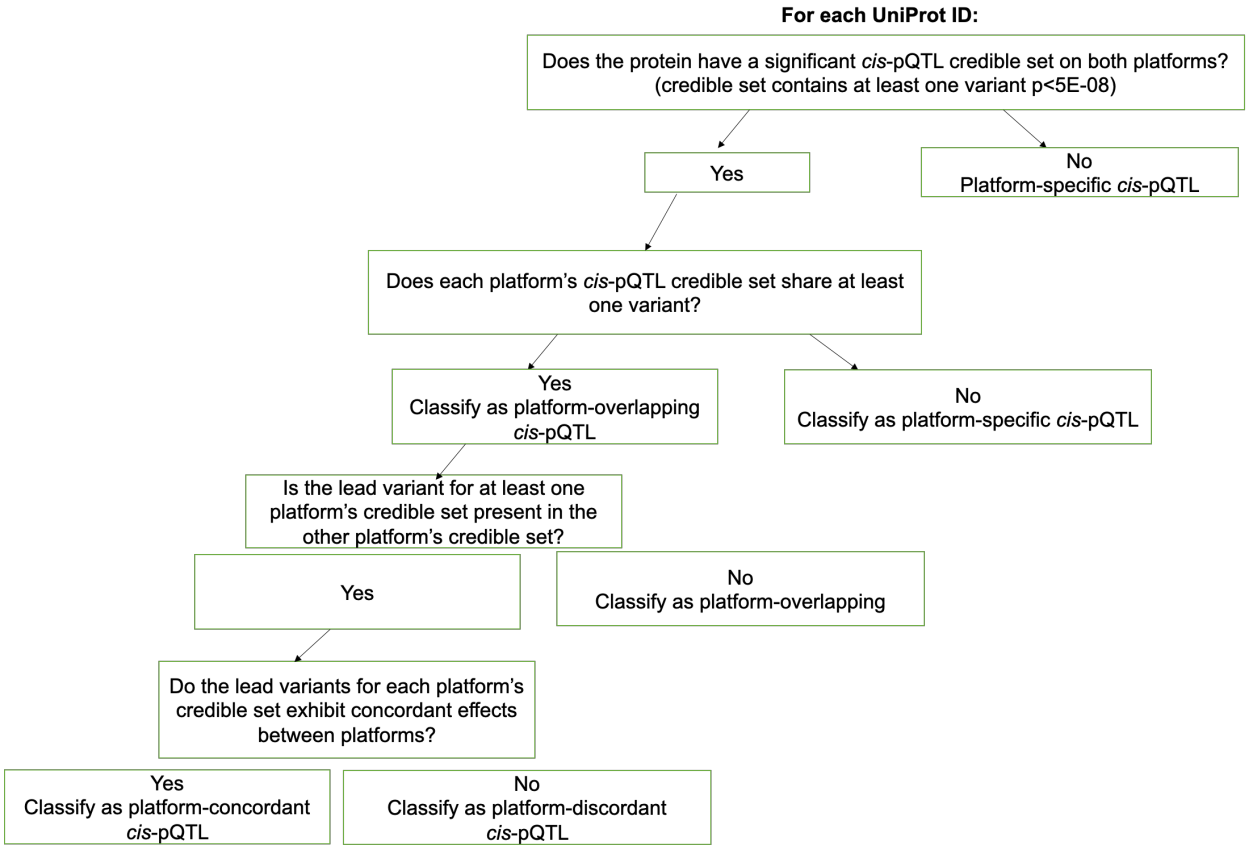

Supplemental Figure 4. Flowchart depicting method for classifying SomaScan and Olink *cis*-pQTL credible sets as platform-concordant, platform-discordant, platform-overlapping, or platform-specific.

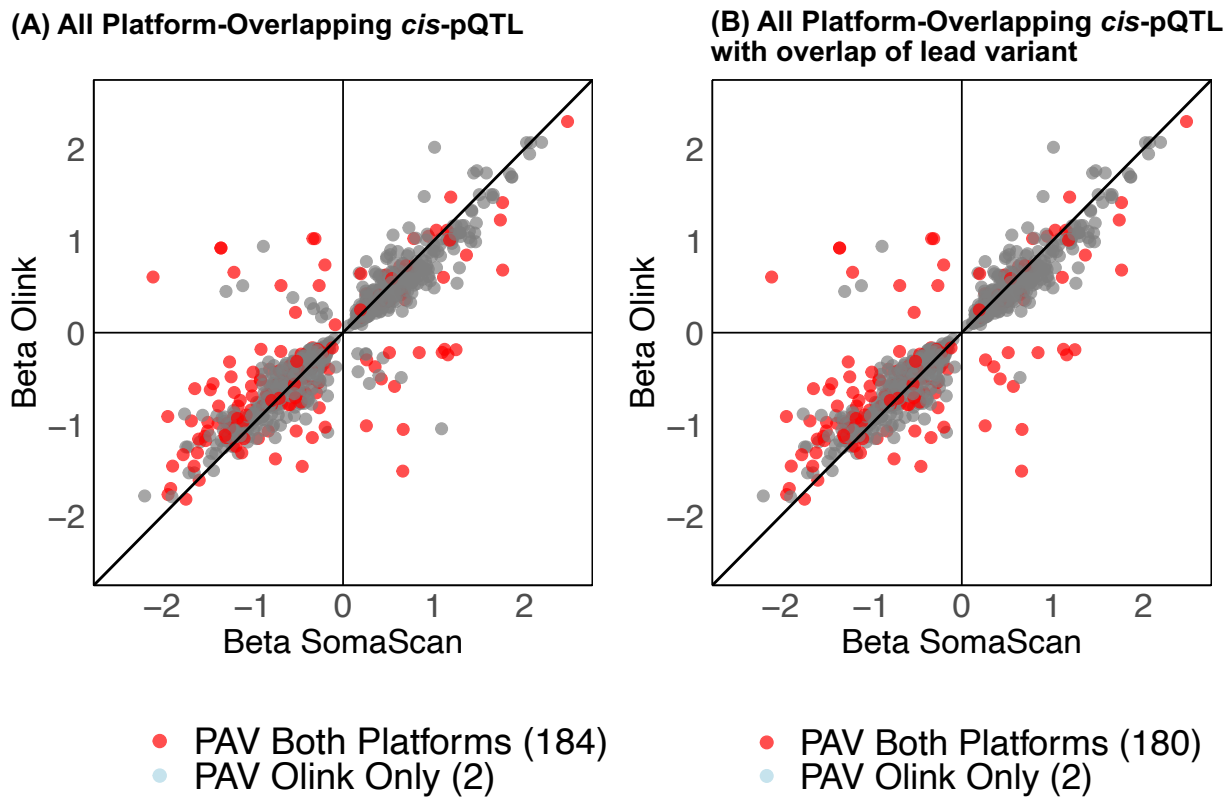

Supplemental Figure 5. Sentinel variant *cis*-pQTL effect-size comparison for all platform-overlapping *cis*-pQTL identified in analysis of all 2,708 probe pairs, with points colored according to whether a PAV for the protein-encoding gene was present in one or both credible sets.

(A) Effect-size comparison across all platform-overlapping credible sets.

(B) Effect-size comparison across platform-overlapping credible sets for which at least one platform's lead variant shared.

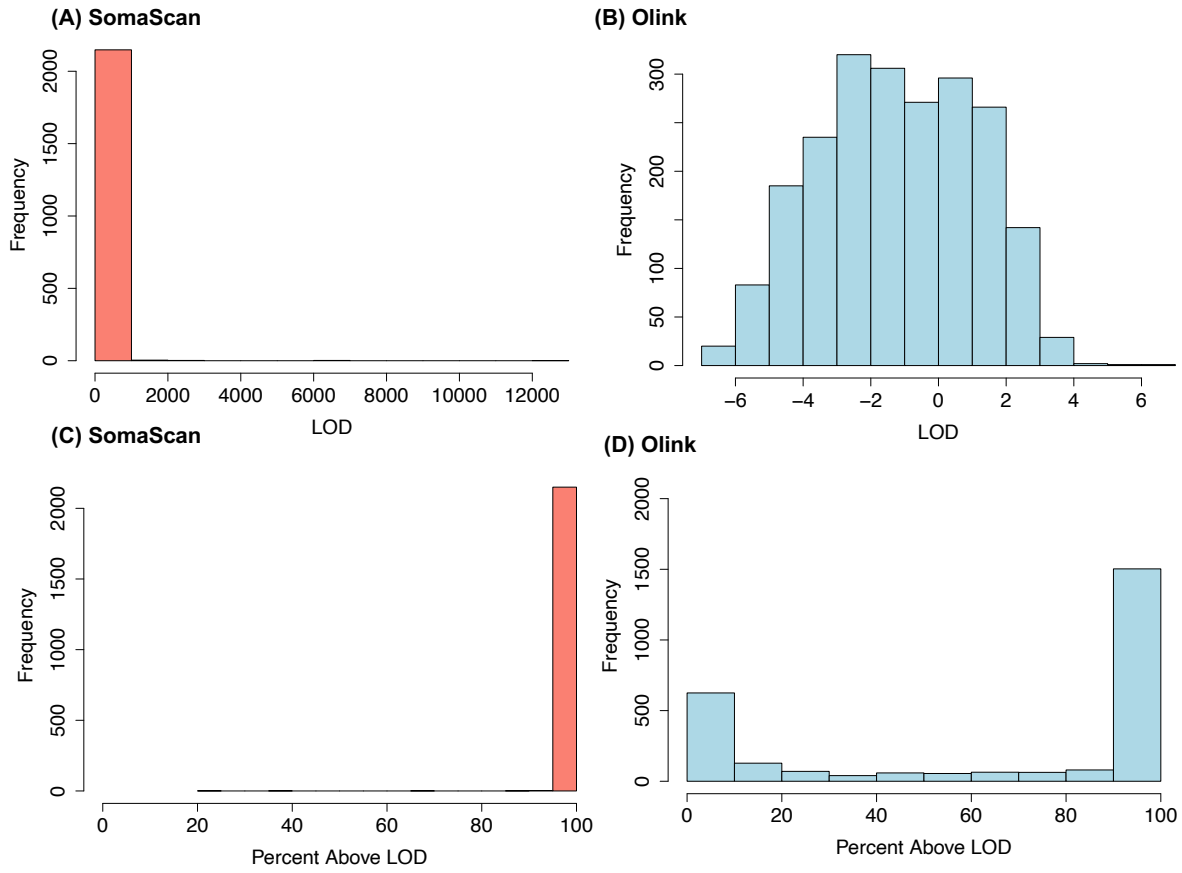

Supplemental Figure 6. (Top panel) Global limit of detection (LOD) values (A) for SomaScan 7k (company-reported values used to define LOD) and (B) for Olink Explore 3072 (calculated from negative controls per company-recommended equation, see methods).

(Bottom panel) For each of the 2,157 proteins compared, histogram displaying the distribution of the percentage of (C) SomaScan measures above the SomaScan LOD and (D) Olink measures above the Olink LOD.

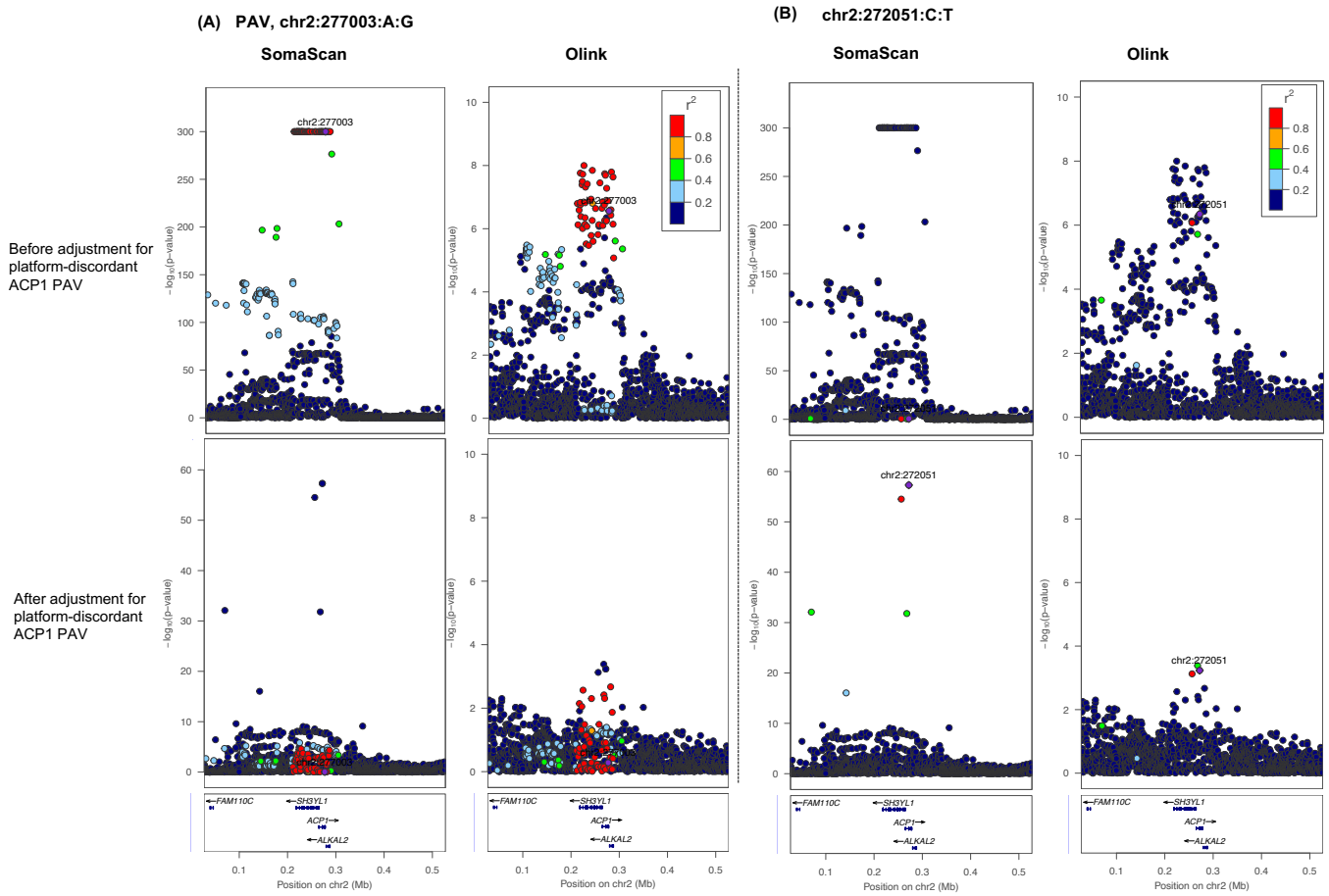

Supplemental Figure 7. Locus Zoom plots displaying the 250KB window around the platform-discordant ACP1 PAV (chr2:277003:A:G) before (top) and after (bottom) adjustment for the platform-discordant PAV on SomaScan vs. Olink. (A) Platform-discordant PAV signal before and after PAV adjustment on SomaScan and Olink, with r^2 values derived in MESA study participants. (B, Top) Before adjustment for the PAV, a second, non-coding signal in the region, led by chr2:272051:C:T, is significantly associated with Olink (right), but not SomaScan (left) ACP1 measures. (B, Bottom) Following adjustment for the platform-discordant PAV, this signal becomes significant on SomaScan. The Y-axes differ in scale between plots.

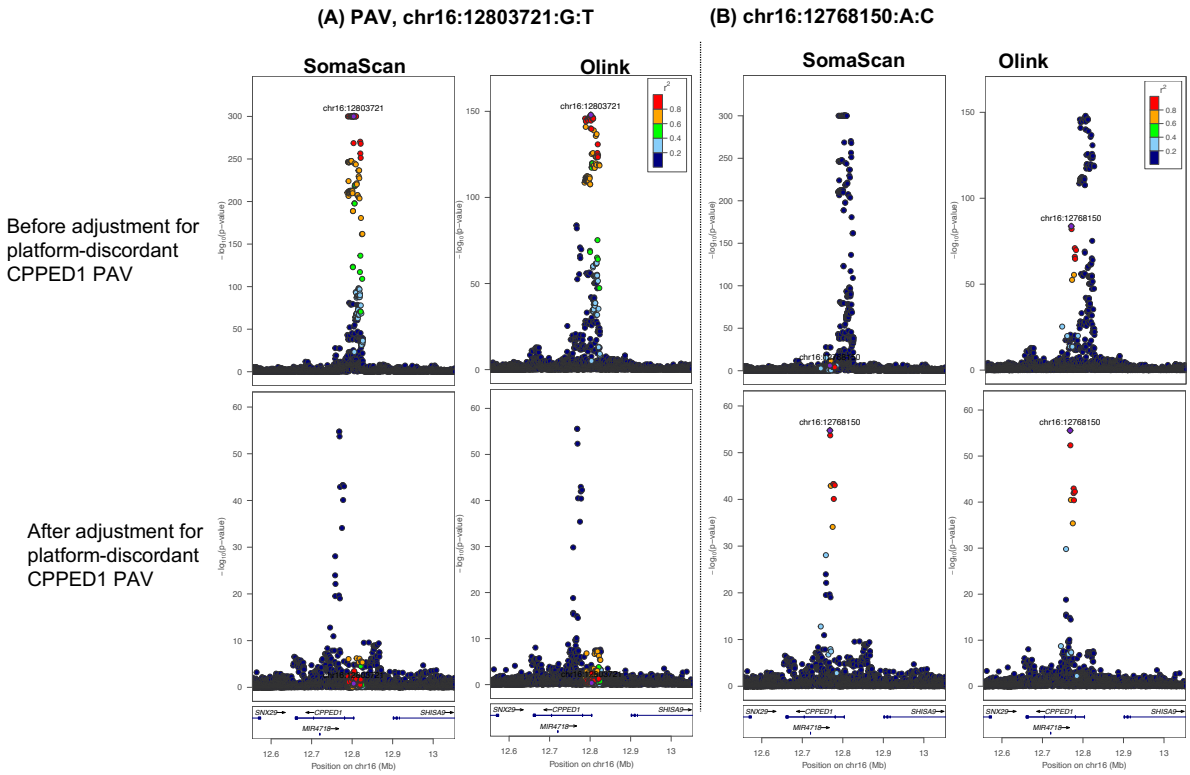

Supplemental Figure 8. Locus Zoom plot displaying the 250KB window around the platform-discordant CPPED1 PAV pre- (top) and post- (bottom) adjustment for the platform-discordant PAV (chr16:12803721:G:T) on SomaScan vs. Olink, with r^2 values derived in MESA study participants. (A) Platform-discordant PAV signal before and after PAV adjustment on SomaScan and Olink. (B, Top) Prior to adjustment for the PAV, a second signal in the region, led by a noncoding variant, chr16:12768150:A:C, is significantly associated with Olink (right), but not SomaScan (left) CPPED1 measures. (B, Bottom) Following adjustment for the platform-discordant PAV, this signal becomes significant on SomaScan. The Y-axes differ in scale between plots.

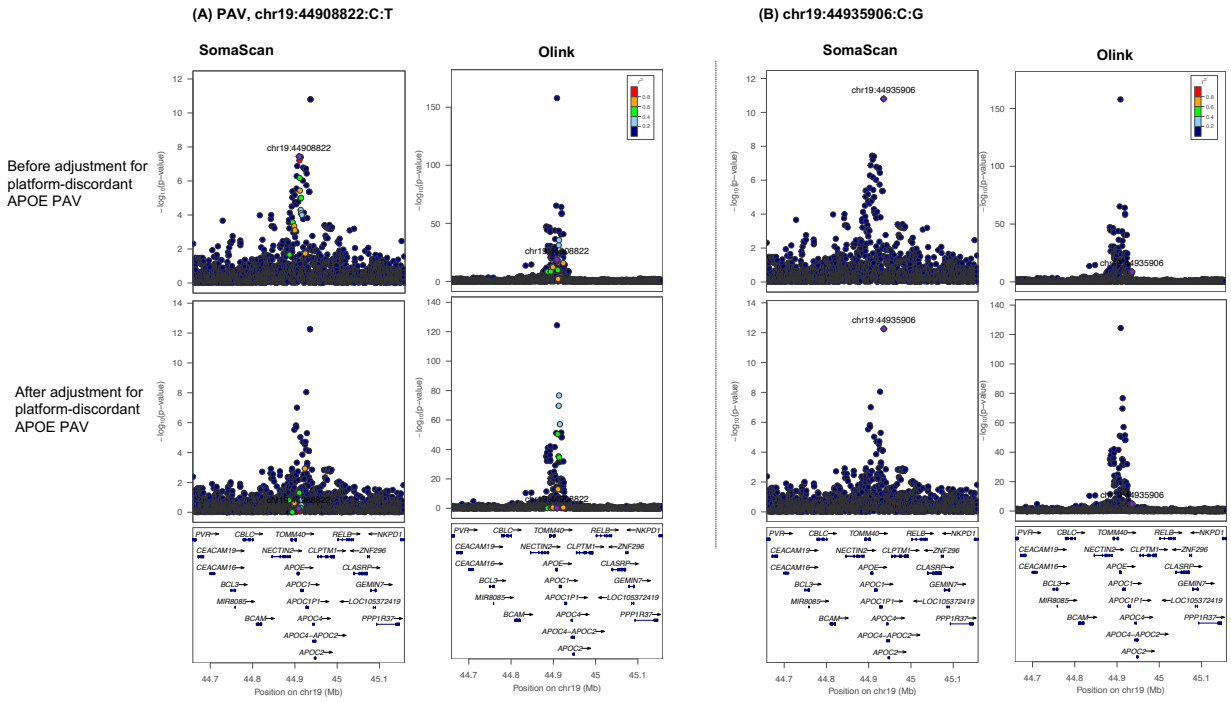

Supplemental Figure 9. Locus Zoom plots displaying the 250KB window around the platform-discordant APOE PAV before (top) and after (bottom) adjustment for the platform-discordant PAV (chr19:44908822:C:T) on SomaScan vs. Olink, with r^2 values derived in MESA study participants. (A) Platform-discordant PAV signal before and after PAV adjustment on SomaScan and Olink. (B) A second signal, driven by noncoding variant chr19:44935906:C:G, is significantly associated with both platforms' APOE measures before adjustment for the platform-discordant PAV. (B, Bottom) Following adjustment for the platform-discordant PAV, this signal increases in significance on SomaScan. The Y-axes differ in scale between plots.

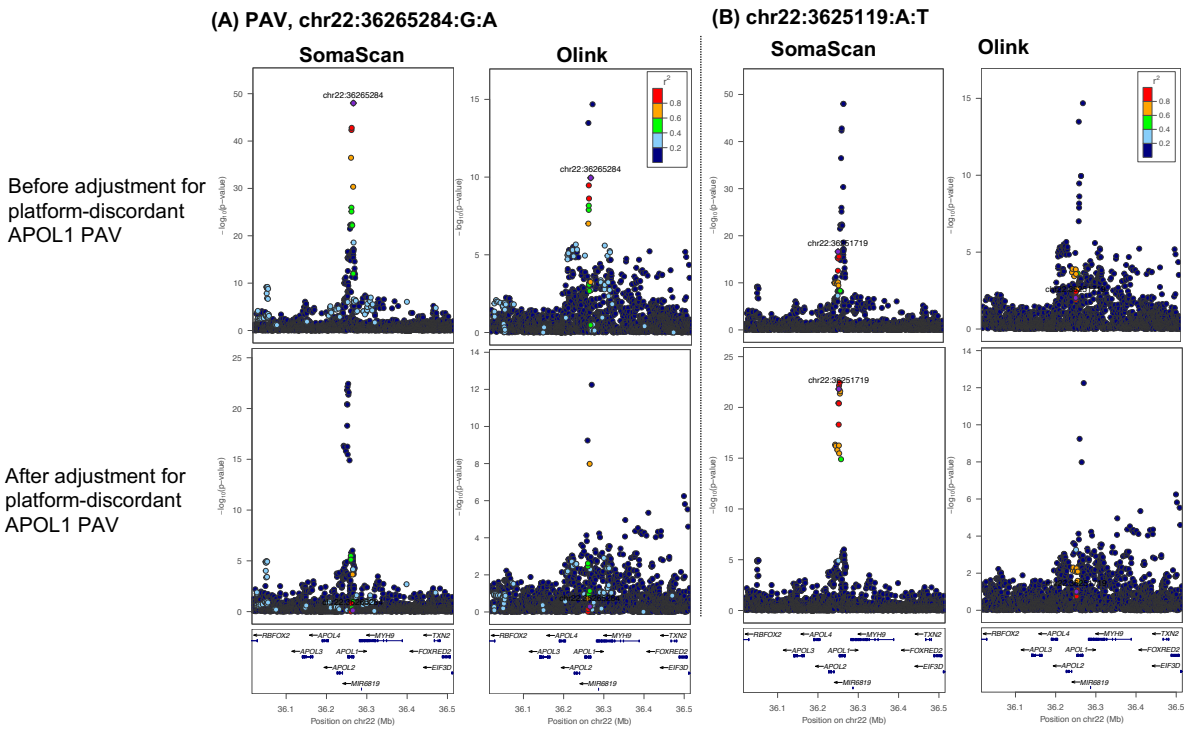

Supplemental Figure 10. Locus Zoom plot displaying the 250KB window around the platform-discordant APOL1 PAV pre- (top) and post- (bottom) adjustment for the platform-discordant PAV (chr22:36265284:G:A) on SomaScan vs. Olink, with r^2 values derived in MESA study participants. (A) Platform-discordant PAV signal before and after PAV adjustment on SomaScan and Olink. (B, Top) Prior to adjustment for the PAV, a second, non-coding signal in the region, led by chr22:3625119:A:T, is significantly associated with SomaScan and Olink APOL1 measures. (B, Bottom) Following adjustment for the platform-discordant PAV, this signal becomes more significant on SomaScan. The Y-axes differ in scale between plots.

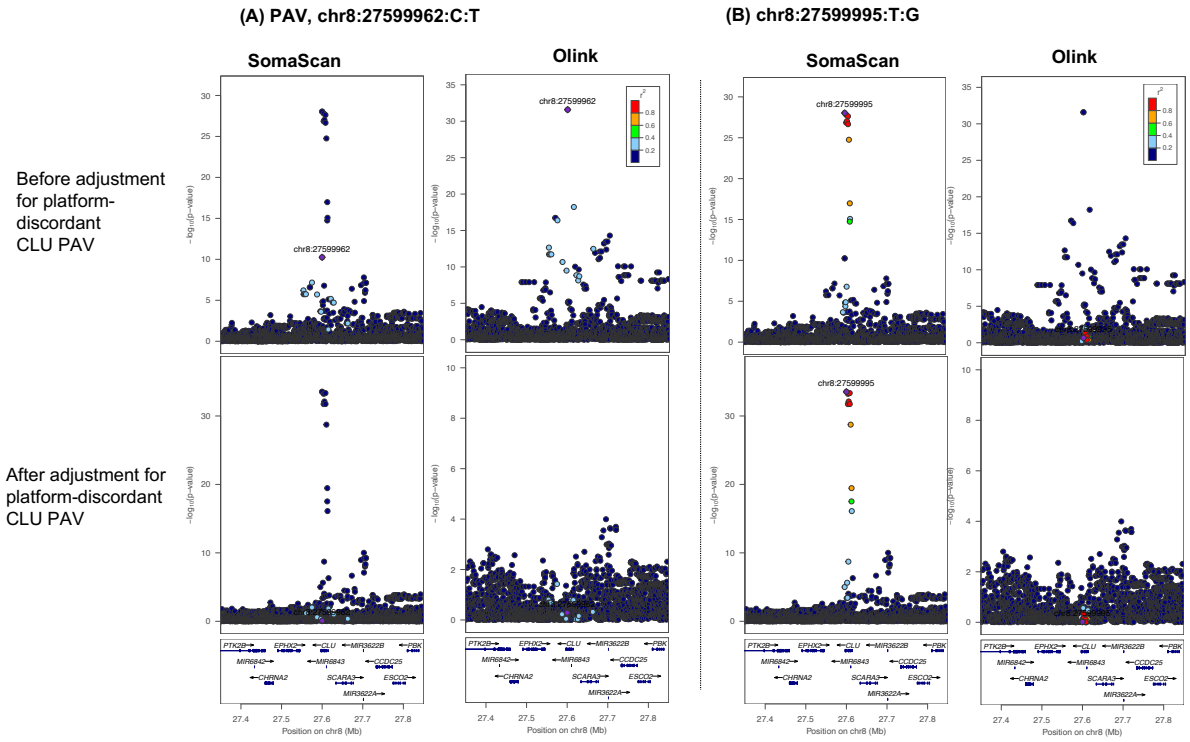

Supplemental Figure 11. Locus Zoom plot displaying the 250KB window around the platform-discordant CLU PAV pre- (top) and post- (bottom) adjustment for the platform-discordant PAV (chr8:27599962:C:T) on SomaScan vs. Olink, with r^2 values derived in MESA study participants. (A) Platform-discordant PAV signal before and after PAV adjustment on SomaScan and Olink. (B) Following adjustment for the platform-discordant PAV, an alternate *cis*-pQTL association, associated with SomaScan CLU measures and led by an independent PAV (chr8:27599995:T:G), increases in significance on SomaScan. The Y-axes differ in scale between plots.

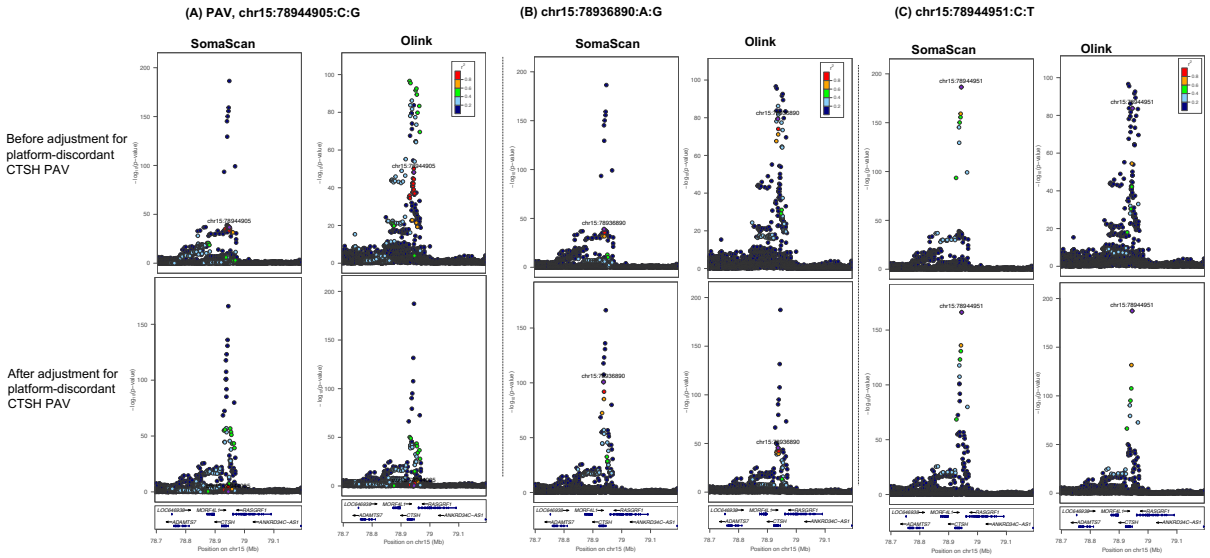

Supplemental Figure 12. Locus Zoom plot displaying the 250KB window around the platform-discordant CTSH PAV pre- (top) and post- (bottom) adjustment for the platform-discordant PAV (chr15:78944905:C:G) on SomaScan vs. Olink. (A) Platform-discordant PAV signal before and after PAV adjustment on SomaScan and Olink, with r^2 values derived in MESA study participants. (B) Following adjustment for the platform-discordant PAV, an alternate *cis*-pQTL association, led by an independent, platform-concordant PAV (chr15:78936890:A:G), positively associated with each platform's measures, increases in significance on SomaScan, but not Olink. (C) Following adjustment for the platform-discordant PAV, a second alternate *cis*-pQTL association, led by another, platform-concordant PAV (chr15:78944951:C:T) negatively associated with each platform's CTSH measures, increases in significance on Olink, but not SomaScan. The Y-axes differ in scale between plots.

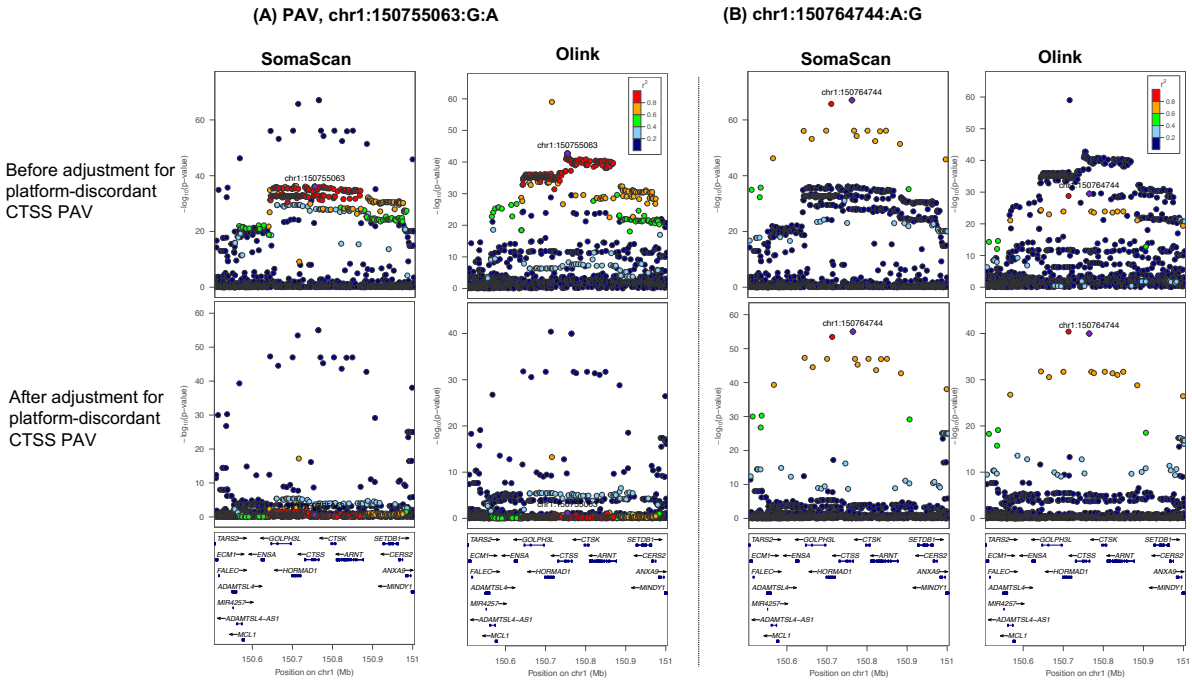

Supplemental Figure 13. Locus Zoom plot displaying the 250KB window around the platform-discordant CTSH PAV pre- (top) and post- (bottom) adjustment for the platform-discordant PAV (chr1:150755063:G:A) on SomaScan vs. Olink, with r^2 values derived in MESA study participants. (A) Platform-discordant PAV signal before and after PAV adjustment on SomaScan and Olink. (B) Following adjustment for the platform-discordant PAV, an alternate *cis*-pQTL association, led by an independent, platform-concordant PAV (chr1:150764744:A:G) that is negatively associated with both platform's CTSS measures, increases in significance on Olink, but not SomaScan. The Y-axes differ in scale between plots.

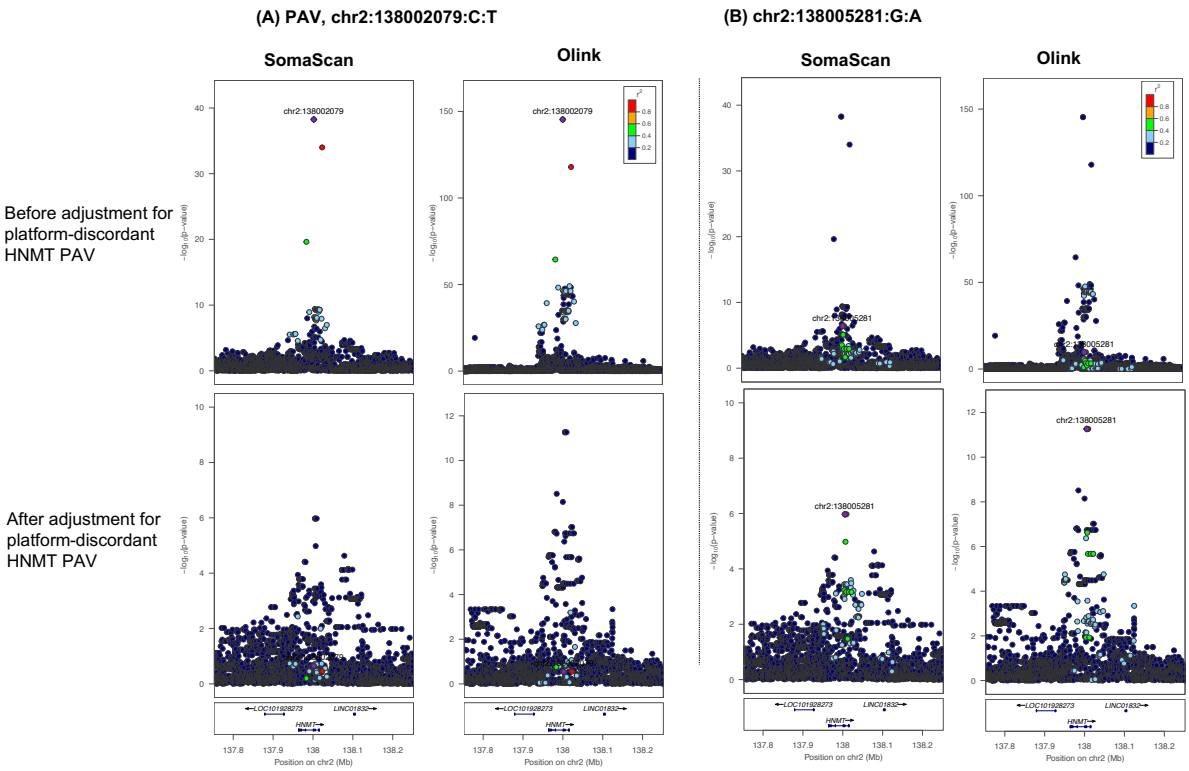

Supplemental Figure 14. Locus Zoom plot displaying the 250KB window around the platform-discordant CTSH PAV pre- (top) and post- (bottom) adjustment for the platform-discordant PAV (chr2:138002079:C:T) on SomaScan vs. Olink, with r^2 values derived in MESA study participants. (A) Platform-discordant PAV signal before and after PAV adjustment on SomaScan and Olink. (B) Following adjustment for the platform-discordant PAV, an alternate *cis*-pQTL association, led by a non-coding variant (chr2:138005281:G:A) that is significantly associated with Olink's HNMT measures, increases in significance on Olink, but not SomaScan. The Y-axes differ in scale between plots.

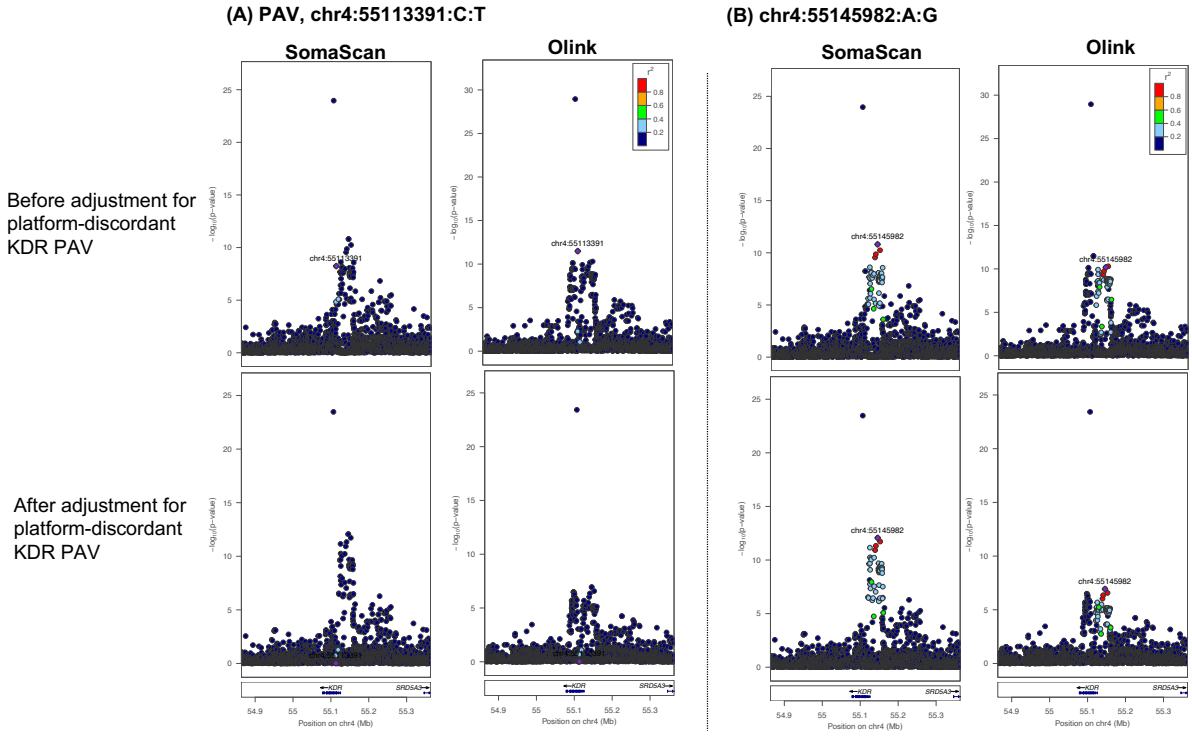

Supplemental Figure 15. Locus Zoom plot displaying the 250KB window around the platform-discordant KDR PAV pre- (top) and post- (bottom) adjustment for the platform-discordant PAV (chr4:55113391:C:T) on SomaScan vs. Olink, with r^2 values derived in MESA study participants. (A) Platform-discordant PAV signal before and after PAV adjustment on SomaScan and Olink. (B) Following adjustment for the platform-discordant PAV, an alternate *cis*-pQTL association, led by an alternate, non-coding variant (chr4:55145982:A:G), increases in significance on SomaScan, but not Olink. The Y-axes differ in scale between plots.

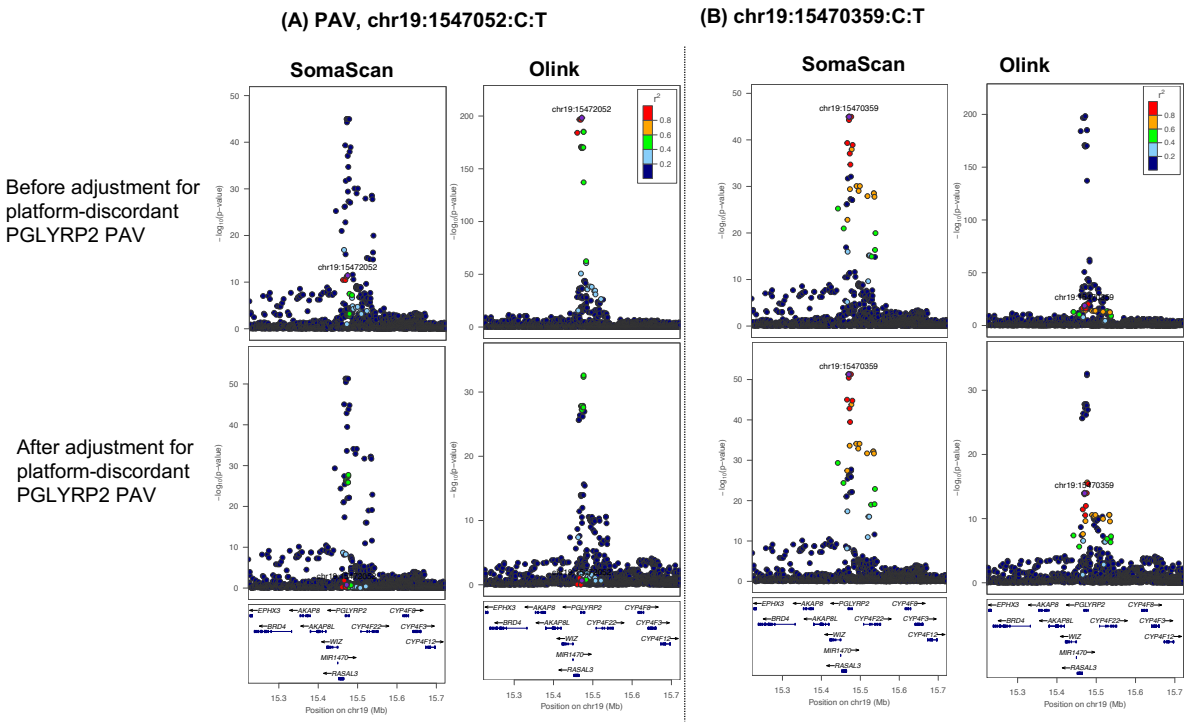

Supplemental Figure 16. Locus Zoom plot displaying the 250KB window around the platform-discordant PGLYRP2 PAV pre- (top) and post- (bottom) adjustment for the platform-discordant PAV (chr19:1547052:C:T) on SomaScan vs. Olink, with r^2 values derived in MESA study participants. (A) Platform-discordant PAV signal before and after PAV adjustment on SomaScan and Olink. (B) Before PAV adjustment, an alternate signal, led by noncoding variant chr19:15470359:C:T, is significantly associated with both platforms' measures of PGLYRP2 pre-PAV adjustment. This association becomes more significant on SomaScan post-PAV adjustment. The Y-axes differ in scale between plots.

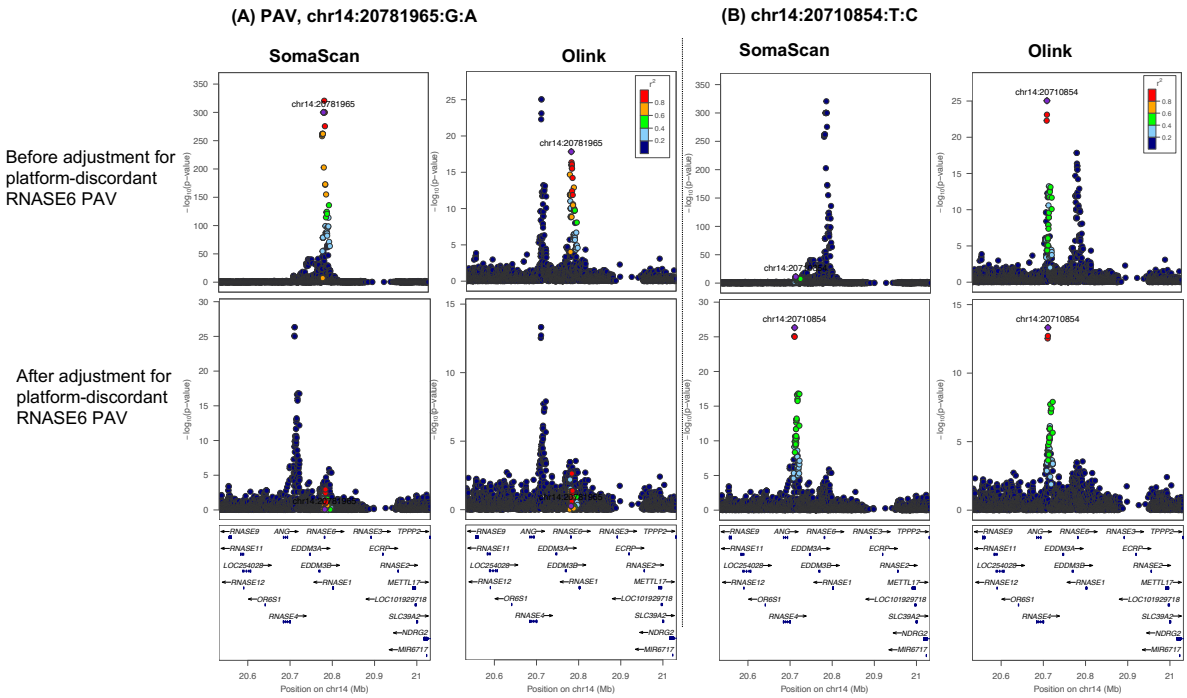

Supplemental Figure 17. Locus Zoom plot displaying the 250KB window around the platform-discordant RNASE6 PAV pre- (top) and post- (bottom) adjustment for the platform-discordant PAV (chr14:20781965:G:A) on SomaScan vs. Olink, with r^2 values derived in MESA study participants. (A) Platform-discordant PAV signal before and after PAV adjustment on SomaScan and Olink. (B) A second signal in the region, led by noncoding variant, chr14:20710854:T:C, is significantly associated with both platforms' RNASE6 measures pre-PAV adjustment. This association increases in significance on SomaScan following PAV adjustment. The Y-axes differ in scale between plots.

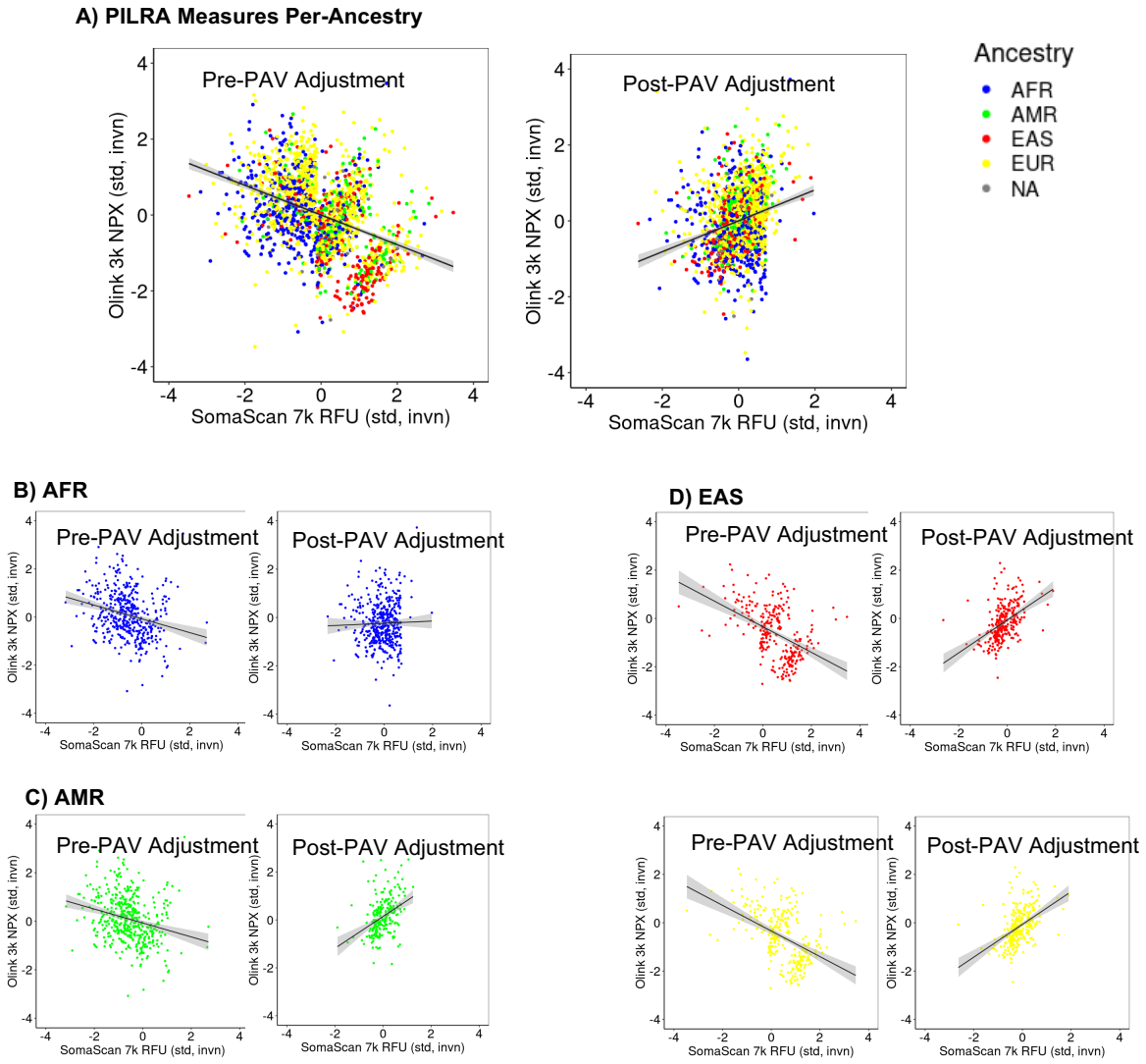

Supplemental Figure 18. (A) SomaScan and Olink PILRA measures pre- (left) and post- (right) PAV adjustment, with points colored by an individual's ancestry cluster. (B-D) SomaScan and Olink measures from individual ancestry reference groups, with lines of best fit with 95% confidence intervals depicted in gray. Correlation improves to the greatest extent among individuals clustering with EAS ancestry references (shown in plot D).

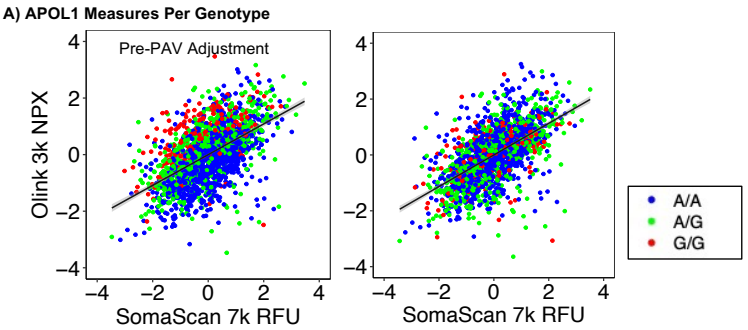

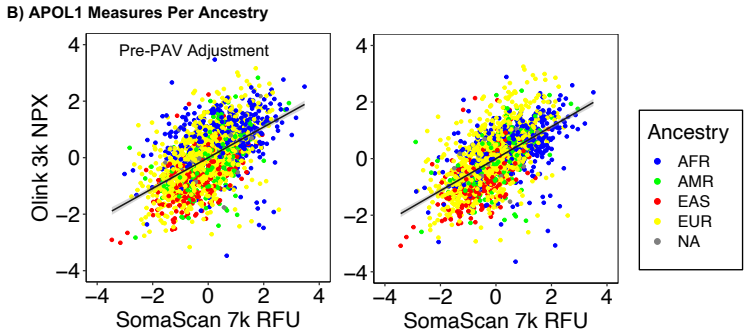

C) rs2239785, chr22:36265284:G:A, Glu166Lys

pQTL Summary Statistics				EAF				
Platform	B	SE	PVAL	AFR	AMR	EAS	EUR	ALL
Soma	0.51	0.034	9.8×10^{-49}	**0.63**	0.14	0.18	0.20	0.29
Olink	-0.21	0.030	1.12×10^{-10}					

D)

	Pearson's r of APOL1 Measures				
	AFR	AMR	EAS	EUR	ALL
Pre-PAV Adjustment	**0.34**	0.55	0.58	0.55	0.54
Post-PAV Adjustment	**0.47**	0.57	0.62	0.60	0.59

Supplemental Figure 19. APOL1 measures pre- (left) and post- (right) adjustment for ancestry differentiated PAV, with points colored (A) by genotype and (B) by ancestry. (C) Ancestry-differentiated PAV summary statistics and effect allele frequencies per-ancestry. Number highlighted in red corresponds to ancestry in which the effect allele is significantly more frequent (here, AFR participants). (D) Pearson's correlation of APOL1 measures per ancestry pre- and post- ancestry differentiated PAV adjustment, with the ancestry group for which highest improvement in inter-platform correlation was observed highlighted in red.

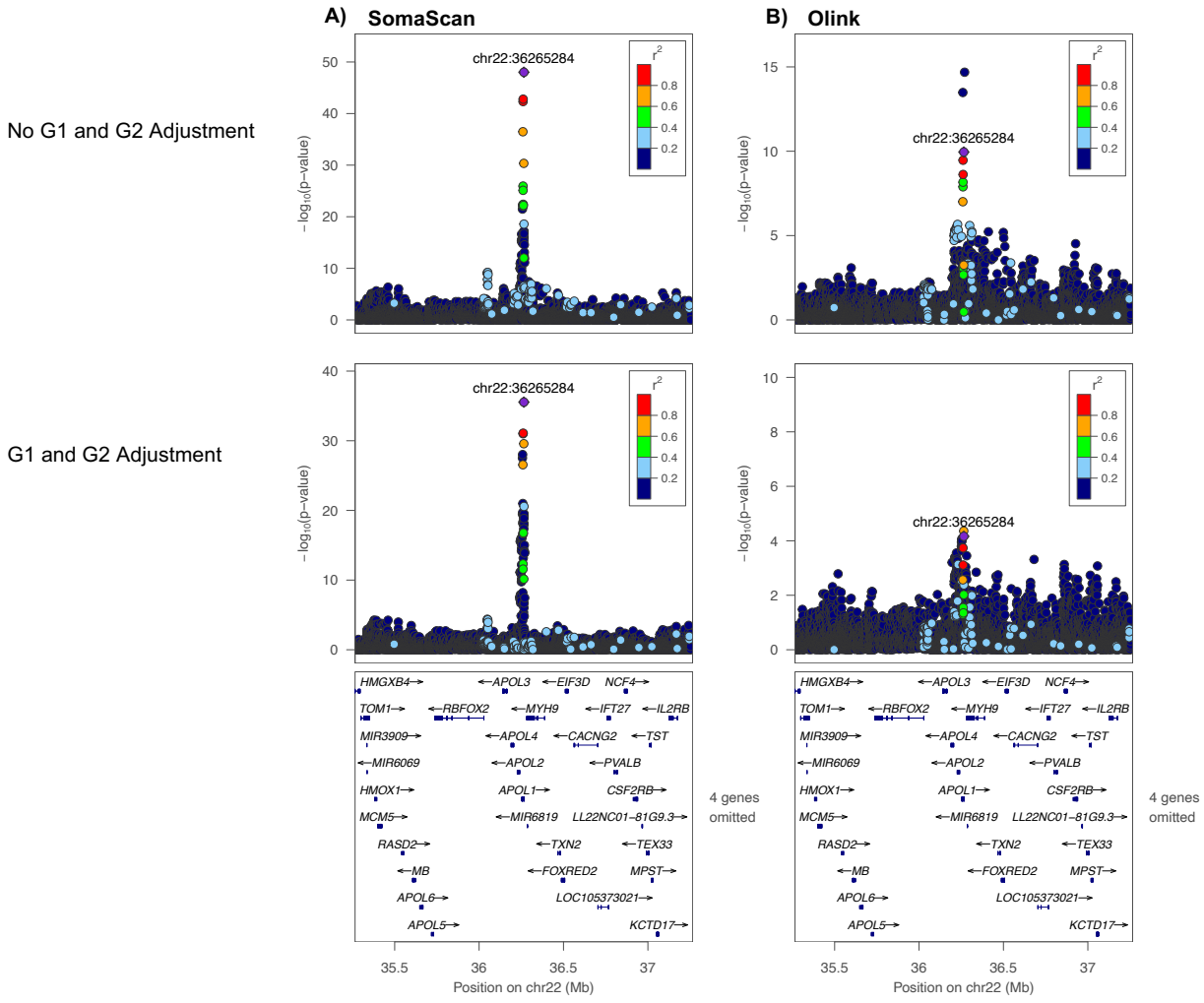

Supplemental Figure 20. Locus Zoom plot displaying the 1MB window around the platform-discordant APOL1 PAV, chr22:36265284:G:A, with r^2 values derived in MESA study participants, before (top plots) and after (bottom plots) adjustment for APOL1 kidney function chronic kidney disease risk variants G1 (rs73885219, chr:36269595:AATAATT:A) and G2 (rs71785313, chr22:36265860:A:G). Platform-discordant PAV signal in APOL1 is attenuated below the significance threshold ($5x10^{-8}$) post-adjustment for the known APOL1 G1 and G2 risk factors, but is still present. The Y axes differ in scale between plots.

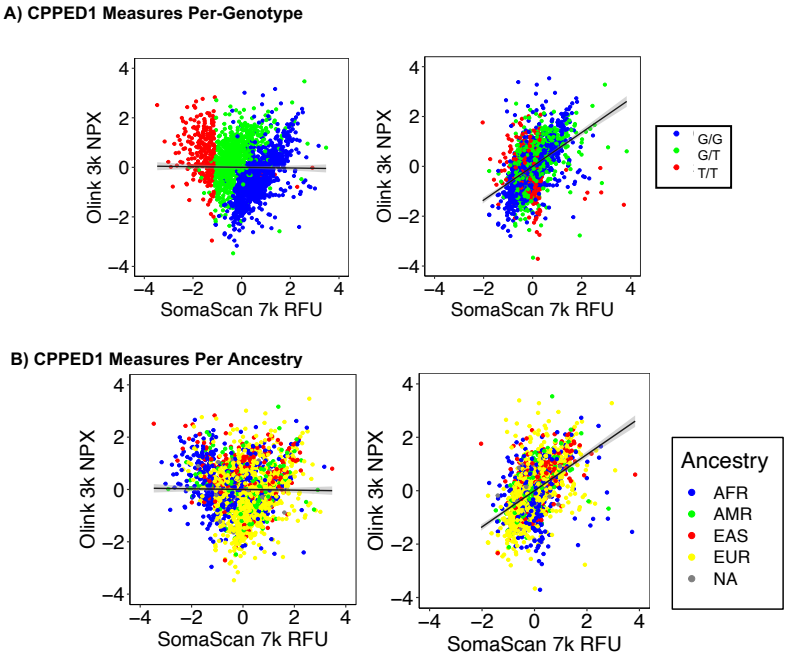

C)

rs3748976, chr16:12803721:G:T, c.A19D

pQTL Summary Statistics				EAF				
Platform	B	SE	PVAL	AFR	AMR	EAS	EUR	ALL
Soma	-1.20	0.023	1.00×10^{-300}	**0.61**	0.28	0.37	0.29	0.33
Olink	0.66	0.02	1.20×10^{-148}					

D)

	Pearson's r of CPPED1 Measures				
	AFR	AMR	EAS	EUR	ALL
Pre-PAV Adjustment	-0.06	-0.06	-0.07	0.13	-0.14
Post-PAV Adjustment	0.27	0.45	0.51	0.56	0.47

Supplemental Figure 21. CPPED1 measures pre- (left) and post- (right) adjustment for ancestry differentiated PAV, with points colored (A) by genotype and (B) by ancestry. (C) Ancestry-differentiated PAV summary statistics and allele frequencies per-ancestry. (D) Pearson's correlation of CPPED1 measures per ancestry pre- and post- ancestry differentiated PAV adjustment.

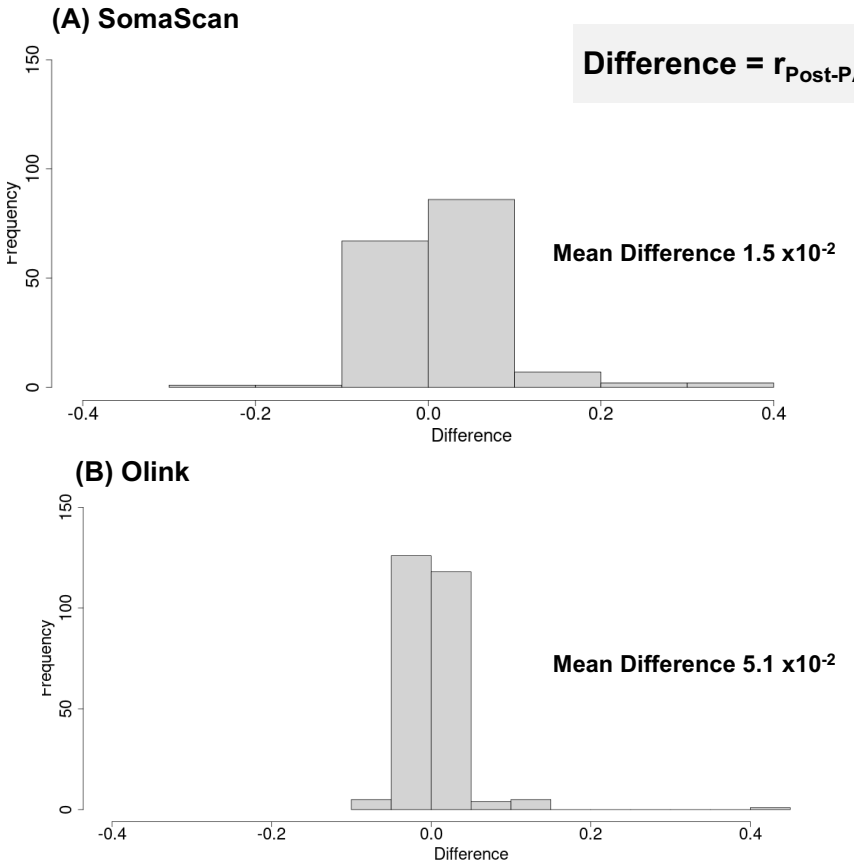

Supplemental Figure 22. Histograms of differences in inter-platform correlation estimates pre- and post- platform-specific PAV adjustment (difference=post-PAV adjusted correlation-pre-PAV adjusted correlation). Difference >0 reflects improved correlation estimate. (A) Adjustment for *cis*-pQTL PAV significantly associated with SomaScan measures only. 166 probe pairs assessed. Difference >0 for 97 probe pairs. (B) Adjustment for *cis*-pQTL PAV significantly associated with Olink measures only. 256 probe pairs assessed. Difference >0 for 128/256 probe pairs.

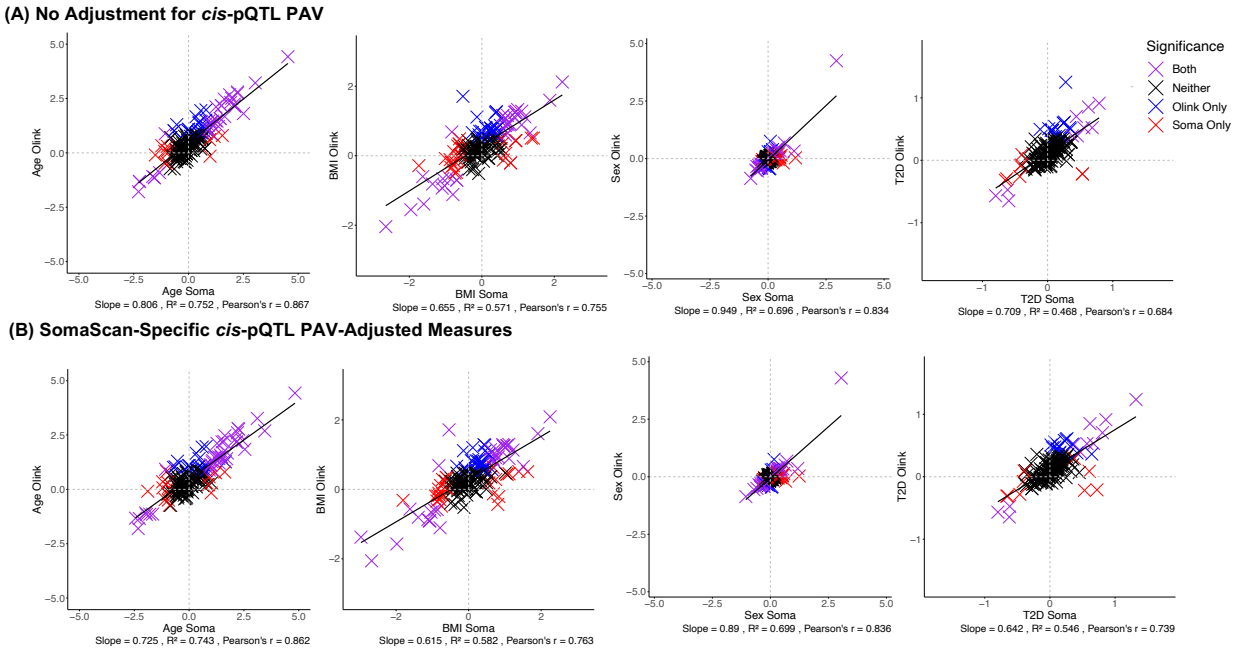

Supplemental Figure 23. Comparison of SomaScan and Olink effect sizes from phenotypic regressions of protein measures with age, sex, BMI, and T2D, before and after adjustment for SomaScan "specific" PAVs. Only proteins with a significant PAV-driven *cis*-pQTL on SomaScan are displayed in the plot. (A) Effect sizes obtained from regression of protein measures without adjustment for SomaScan-specific PAVs (B) Effect sizes obtained from regression of SomaScan-"specific" PAV-adjusted protein measures with each phenotype. In both plots, points are colored according to Bonferroni significance ($p<0.05/2,708$) of protein-phenotype association on both platforms (purple), SomaScan only (red), Olink only (blue), or neither platform.

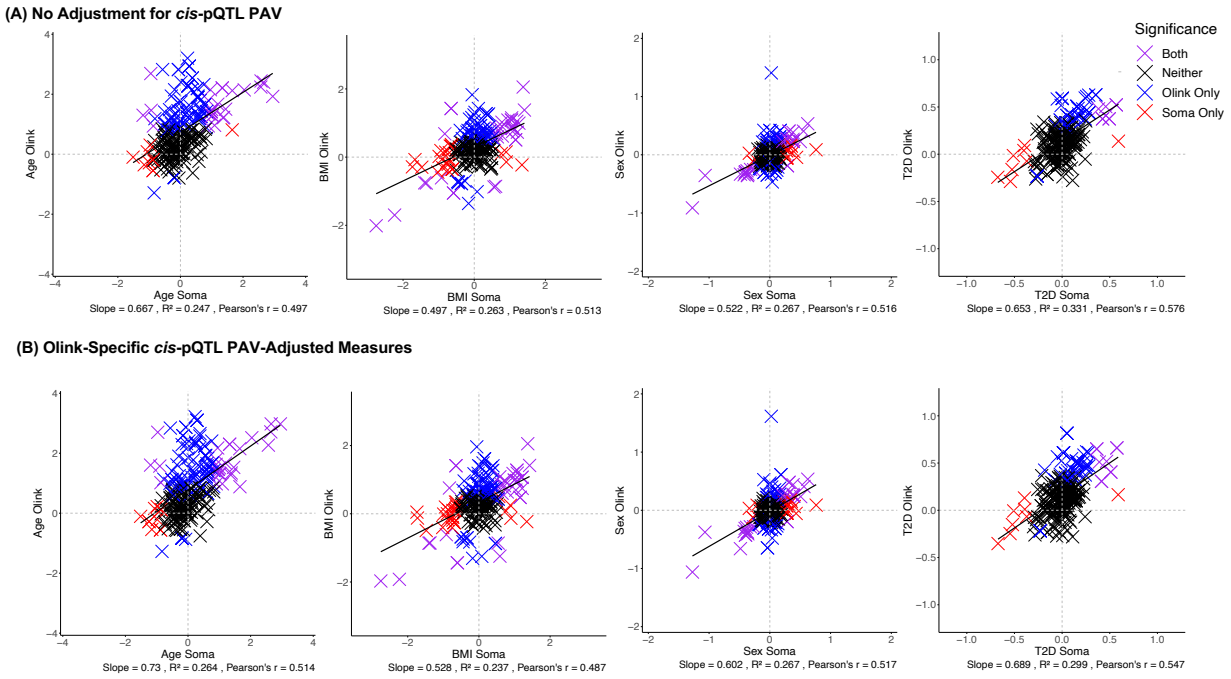

Supplemental Figure 24. Comparison of SomaScan and Olink effect sizes from phenotypic regressions of protein measures with age, sex, body mass index (BMI), and type 2 diabetes (T2D), before and after adjustment for Olink "specific" PAVs. Only proteins with a significant PAV-driven *cis*-pQTL association on Olink are displayed in the plot. (A) Effect sizes obtained from regression of protein measures without adjustment for Olink-specific PAVs (B) Effect sizes obtained from regression of Olink-"specific" PAV-adjusted protein measures with each phenotype. In both plots, points are colored according to Bonferroni significance ($p<0.05/2,708$) of protein-phenotype association on both platforms (purple), SomaScan only (red), Olink only (blue), or neither platform.

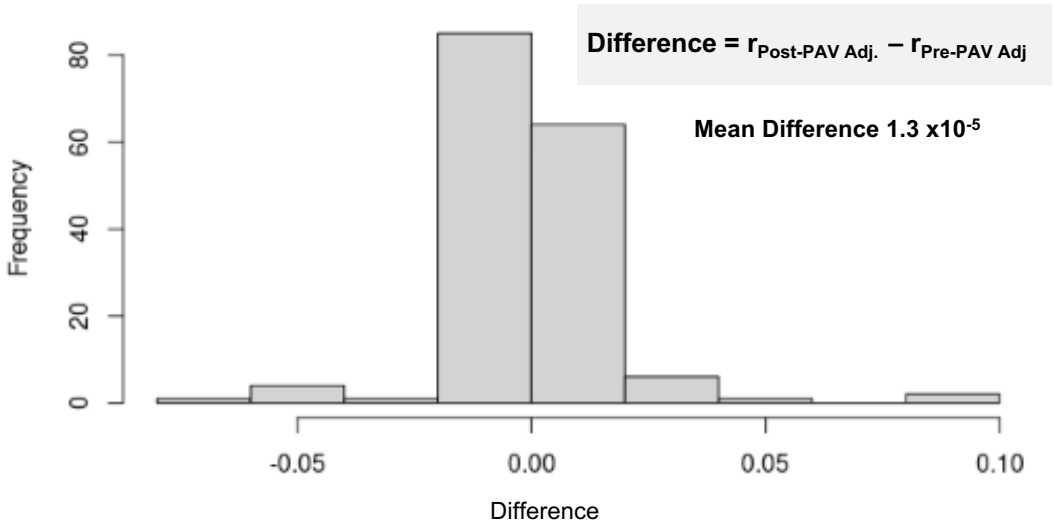

Supplemental Figure 25. Histogram of differences in inter-platform Pearson's correlation estimates pre- and post- adjustment for lead *trans*-pQTL variants in SomaScan-specific pleiotropic regions (difference=post-PAV adjusted correlation-pre-PAV adjusted correlation). Difference >0 reflects improved correlation estimate.

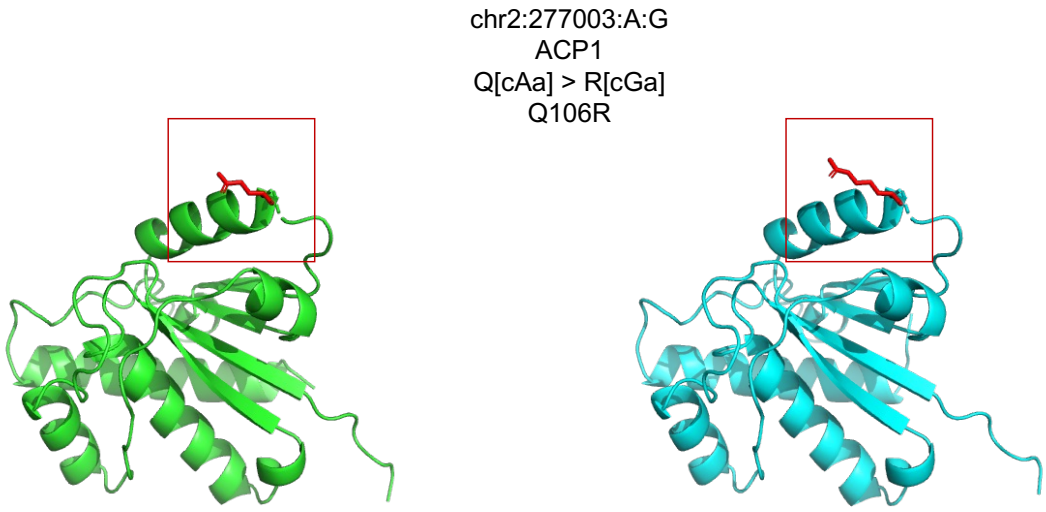

Supplemental Figure 26. Visual representation of predicted consequences of ACP1 platform-discordant PAV.

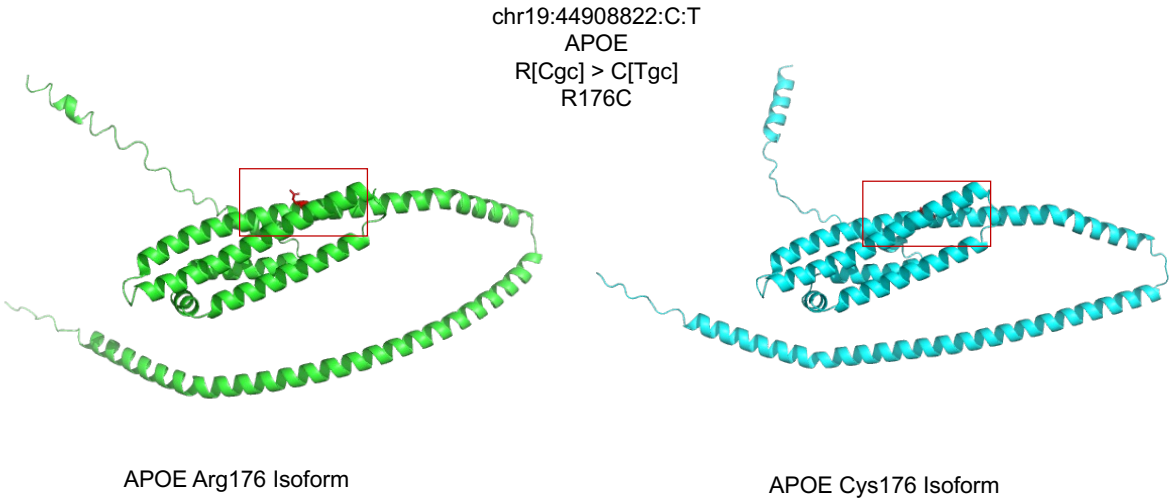

Supplemental Figure 27. Visual representation of predicted consequences of APOE platform-discordant PAV.

chr22:36265284:G:A
APOL1
E[Gag] > K[Aag]
E166K

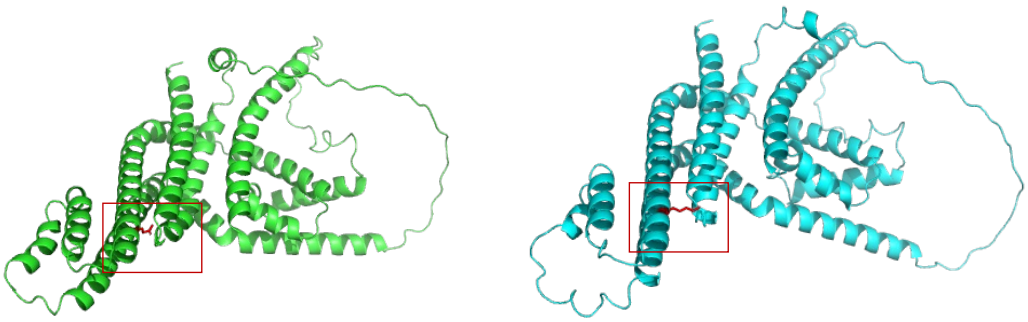

APOL1 Glu166 Isoform

APOL1 Lys166 Isoform

746
747 **Supplemental Figure 28.** Visual representation of predicted consequences of
748 APOL1 platform-discordant PAV.
749
750

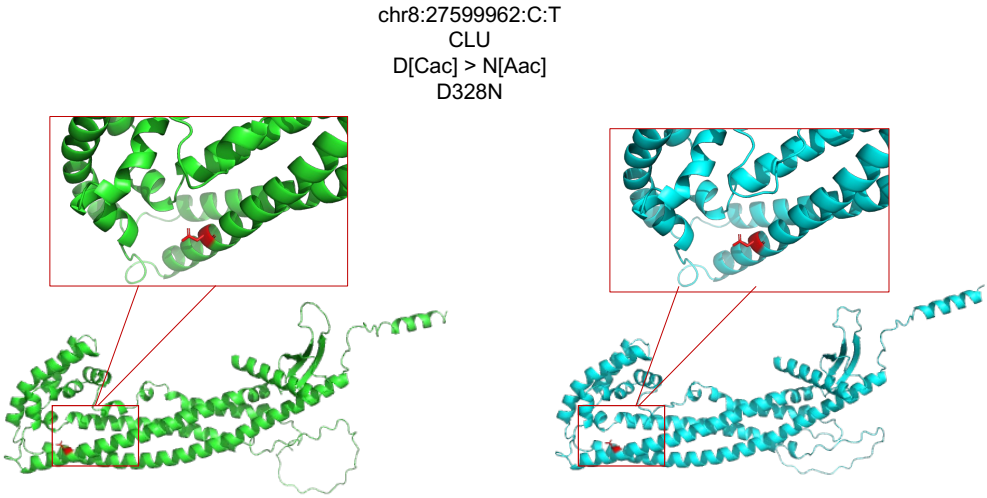

Supplemental Figure 29. Visual representation of predicted consequences of CLU platform-discordant PAV.

chr16:12803721:G:T
CPPED1
A[gGc] > D[gTc]
A19V

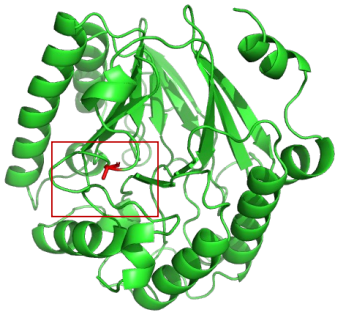

CPPED1 Ala19 Isoform

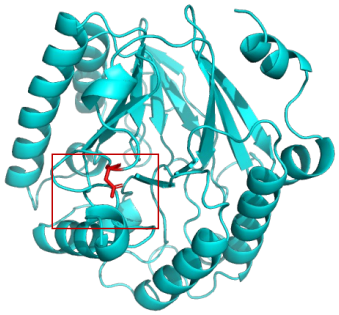

CPPED1 Asp19 Isoform

Supplemental Figure 30. Visual representation of predicted consequences of CPPED1 platform-discordant PAV.

chr15:78944905:C:G
CTSH
C[tCc] > S[tGc]
C26S

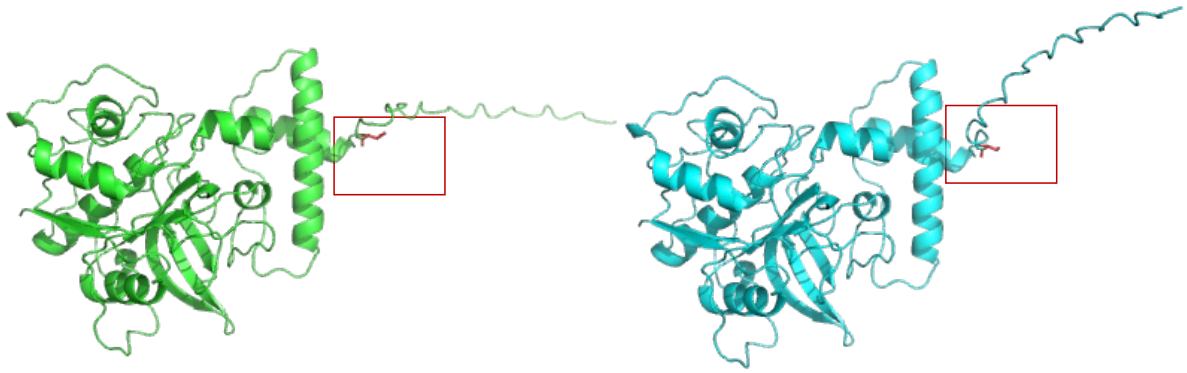

CTSH Cys26 Isoform

CTSH Ser26 Isoform

Supplemental Figure 31. Visual representation of predicted consequences of CTSH platform-discordant PAV.

chr1:150755063:G:A
CTSS
R[Ggg] > W[Agg]
R113W

CTSS Arg113 Isoform

CTSS Trp113 Isoform

Supplemental Figure 32. Visual representation of predicted consequences of CTSS platform-discordant PAV.

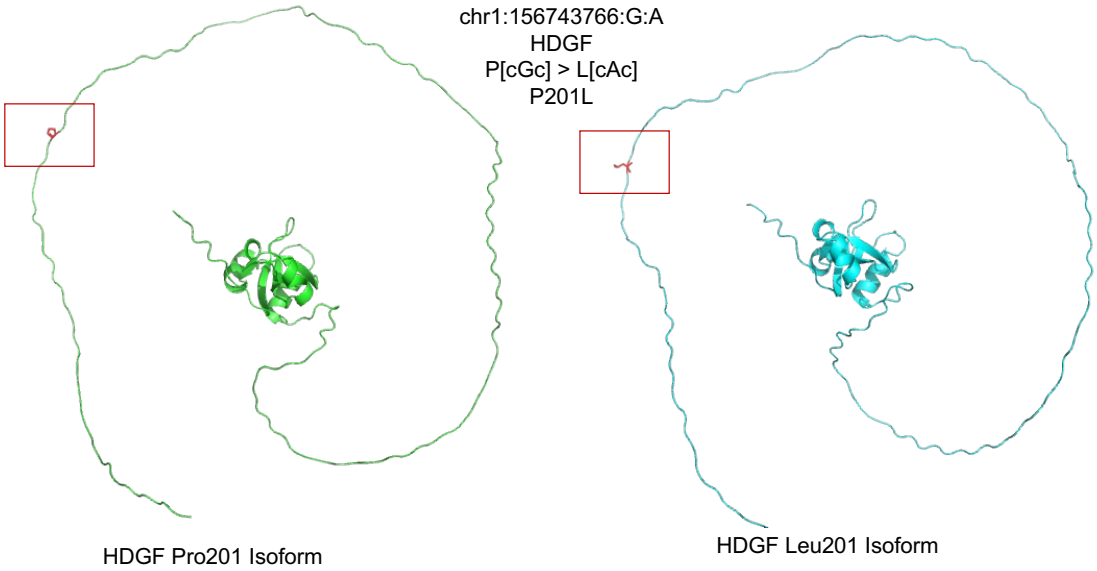

Supplemental Figure 33. Visual representation of predicted consequences of HDGF platform-discordant PAV.

chr2:138002079:C:T
HNMT
T[aCa] > I[aTa]
T105I

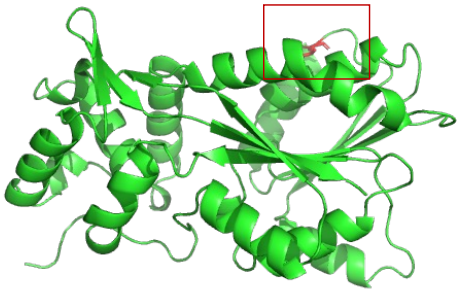

HNMT Thr105 Isoform

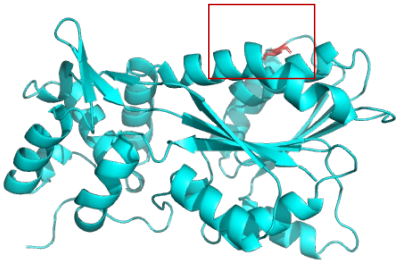

HNMT Ile105 Isoform

Supplemental Figure 34. Visual representation of predicted consequences of HNMT platform-discordant PAV.

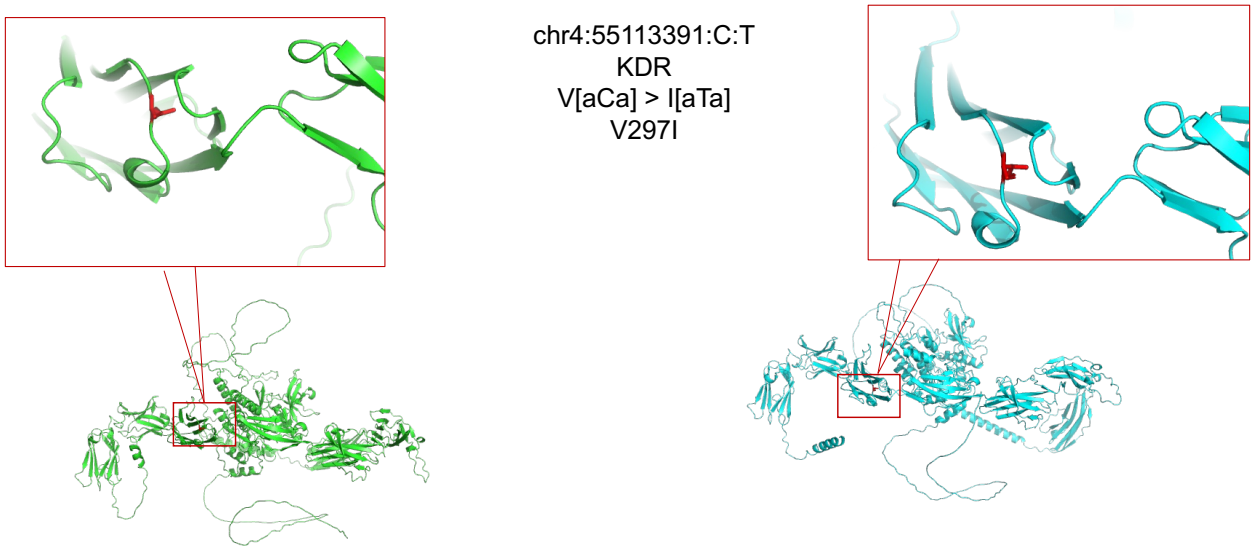

Supplemental Figure 35. Visual representation of predicted consequences of KDR platform-discordant PAV.

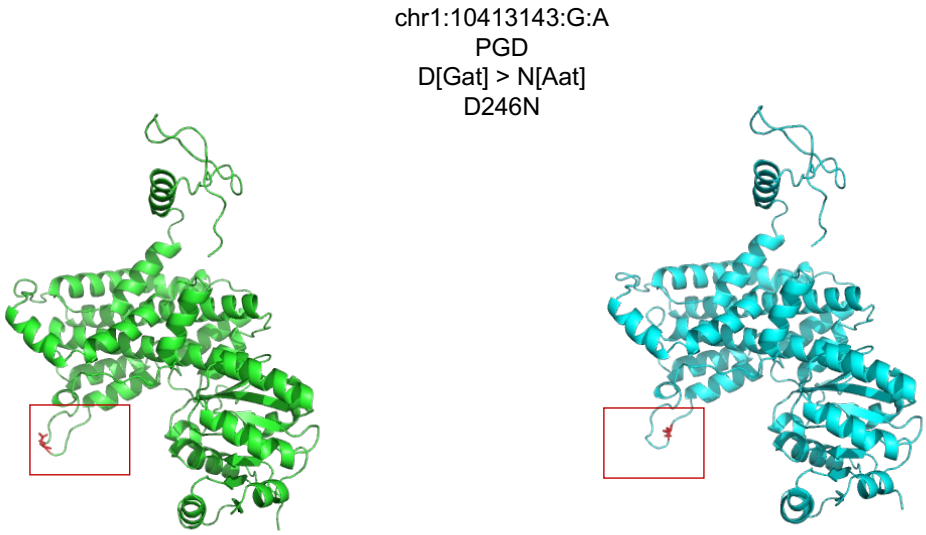

Supplemental Figure 36. Visual representation of predicted consequences of PGD platform-discordant PAV.

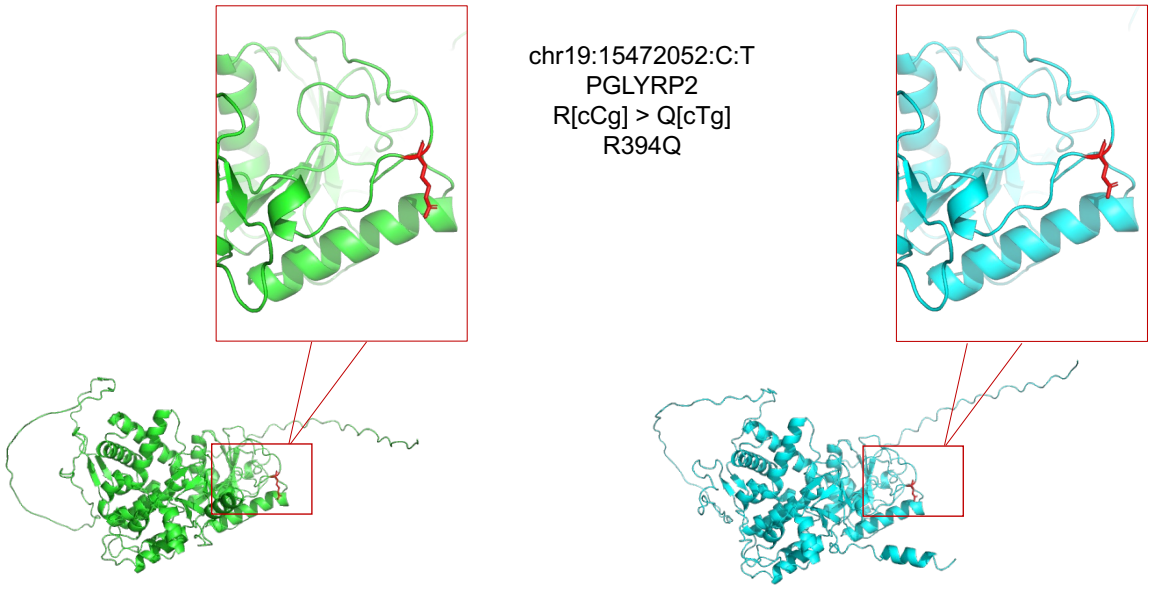

Supplemental Figure 37. Visual representation of predicted consequences of PGLYRP2 platform-discordant PAV.

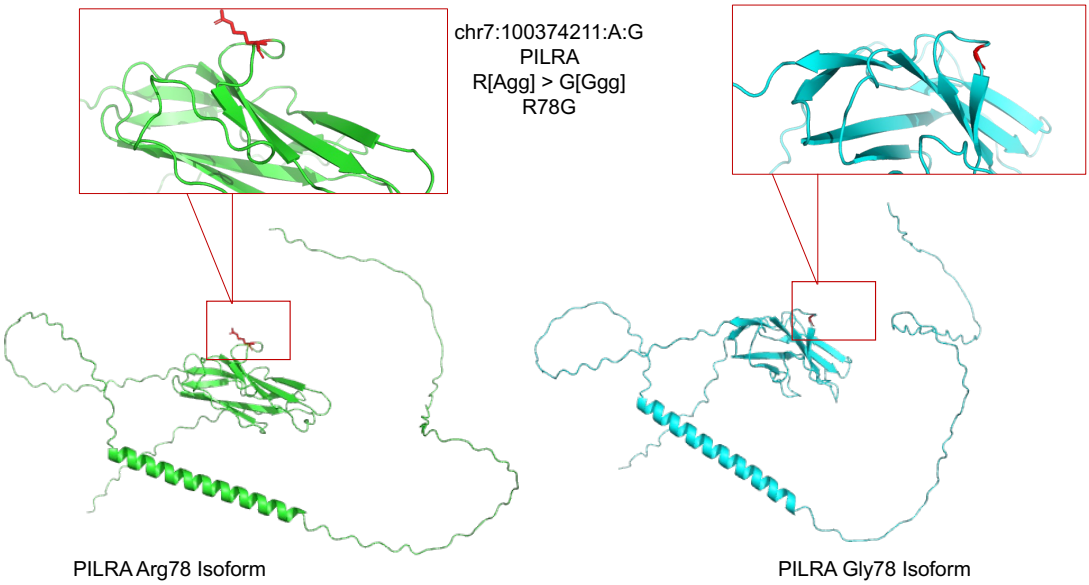

Supplemental Figure 38. Visual representation of predicted consequences of PILRA platform-discordant PAV.

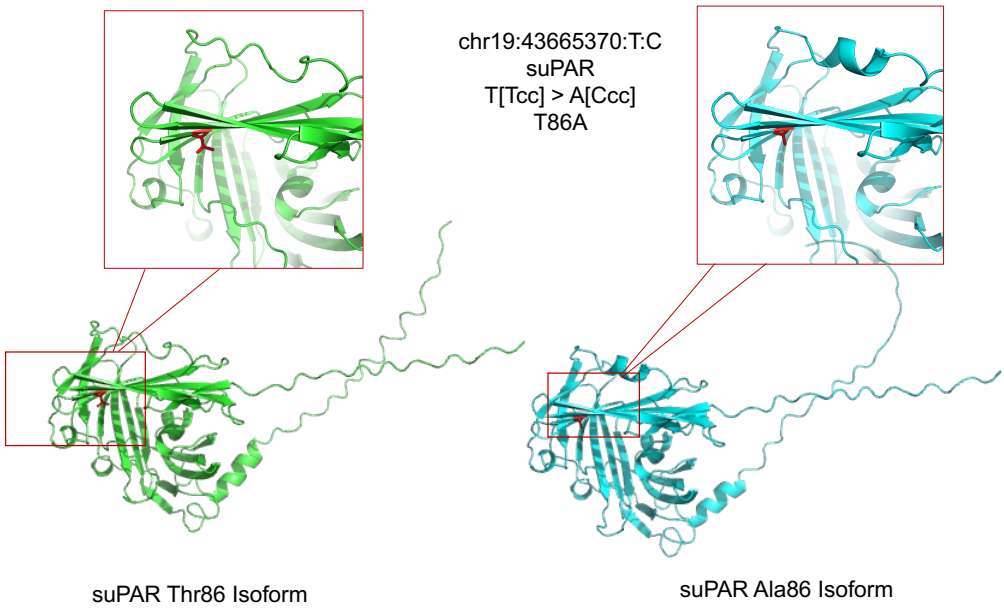

Supplemental Figure 39. Visual representation of predicted consequences of suPAR platform-discordant PAV on suPAR.

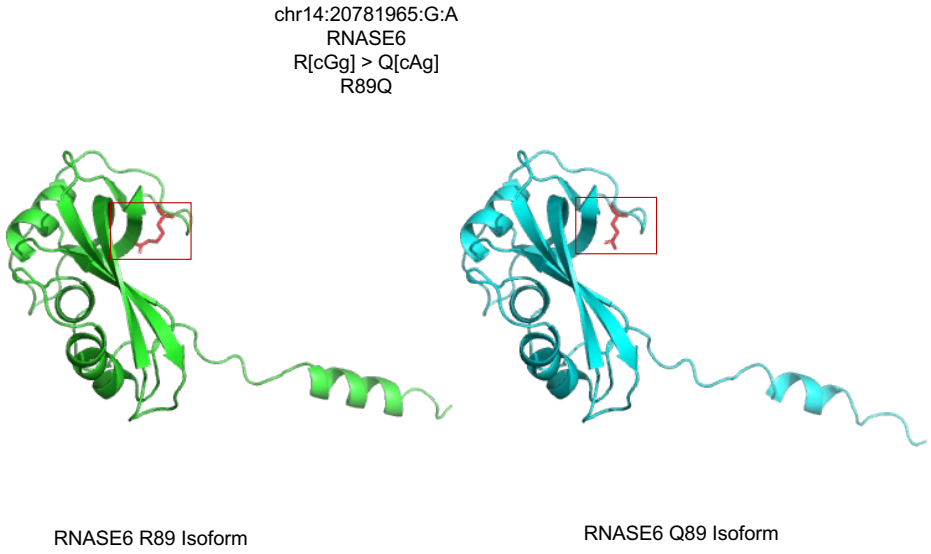

Supplemental Figure 40. Visual representation of predicted consequences of RNASE6 platform-discordant PAV.

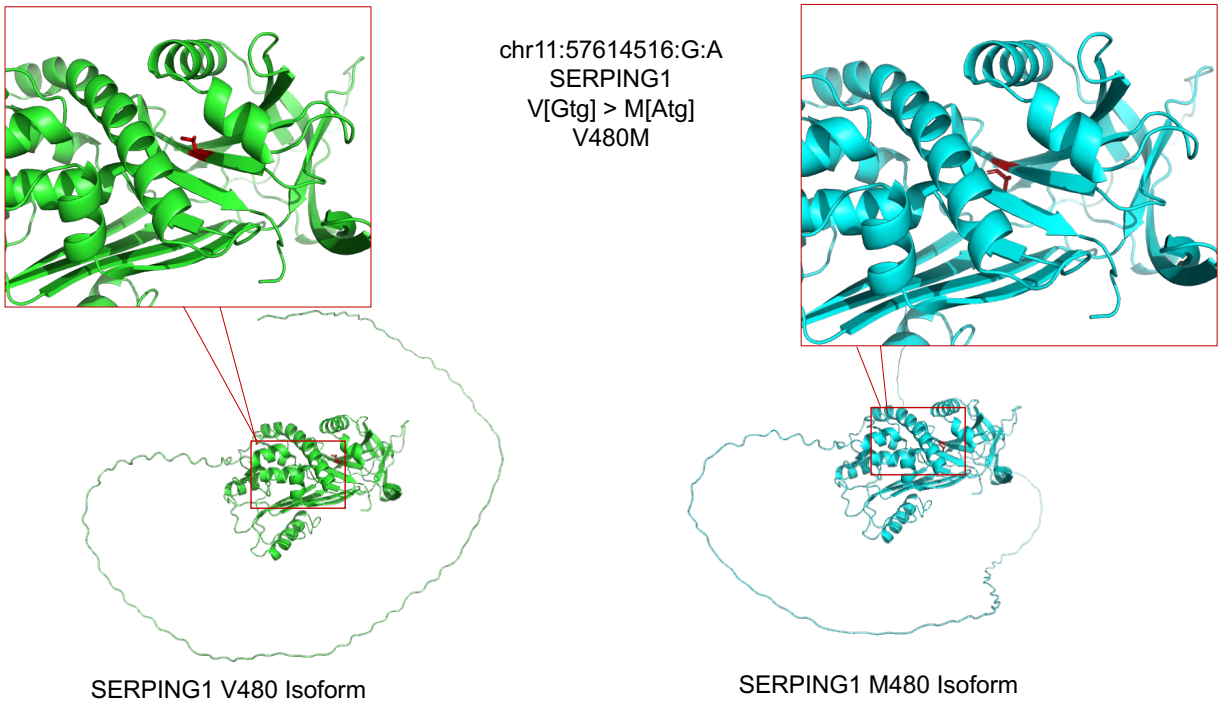

Supplemental Figure 41. Visual representation of predicted consequences of SERPING1 platform-discordant PAV.

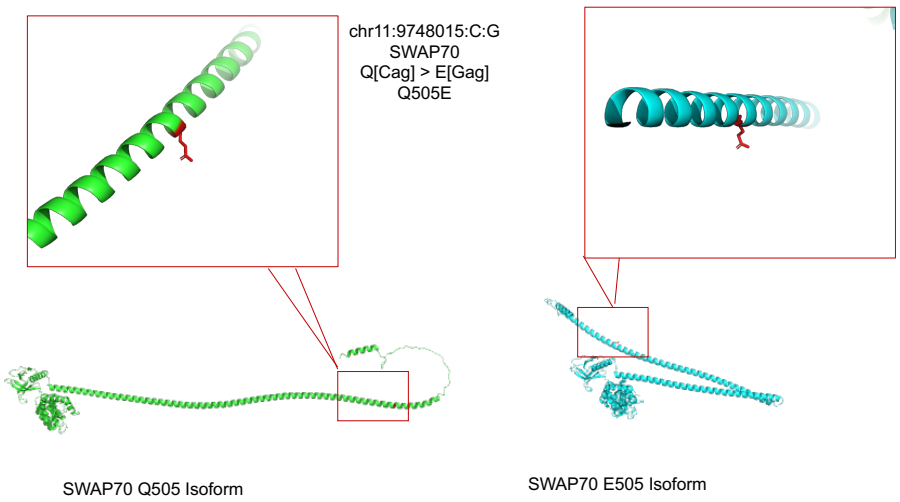

Supplemental Figure 42. Visual representation of predicted consequences of SWAP70 platform-discordant PAV.

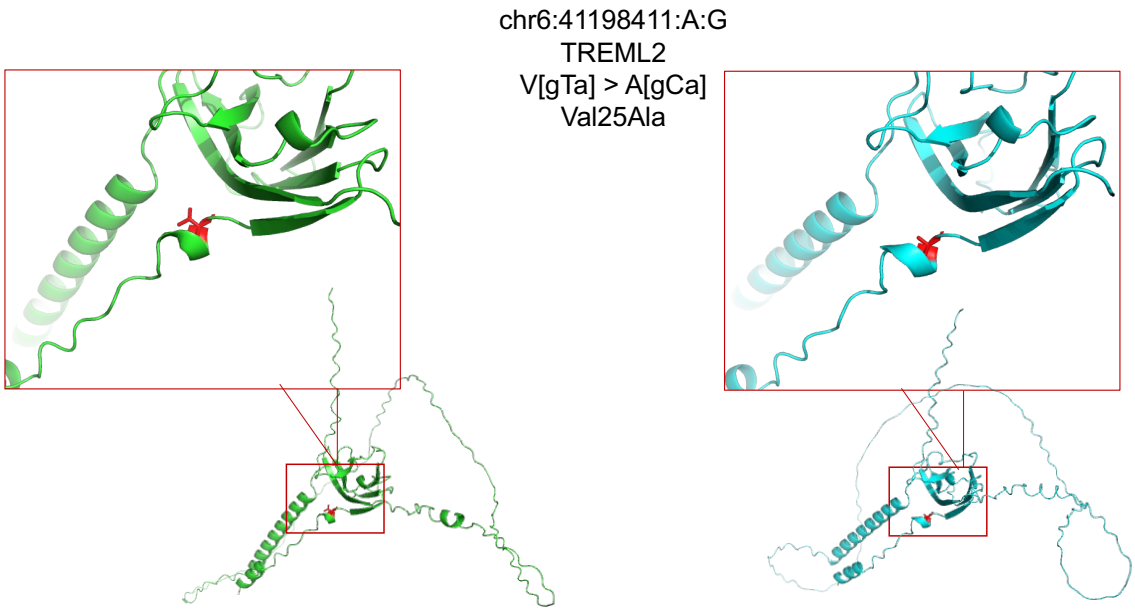

Supplemental Figure 43. Visual representation of predicted consequences of TREML2 platform-discordant PAV.